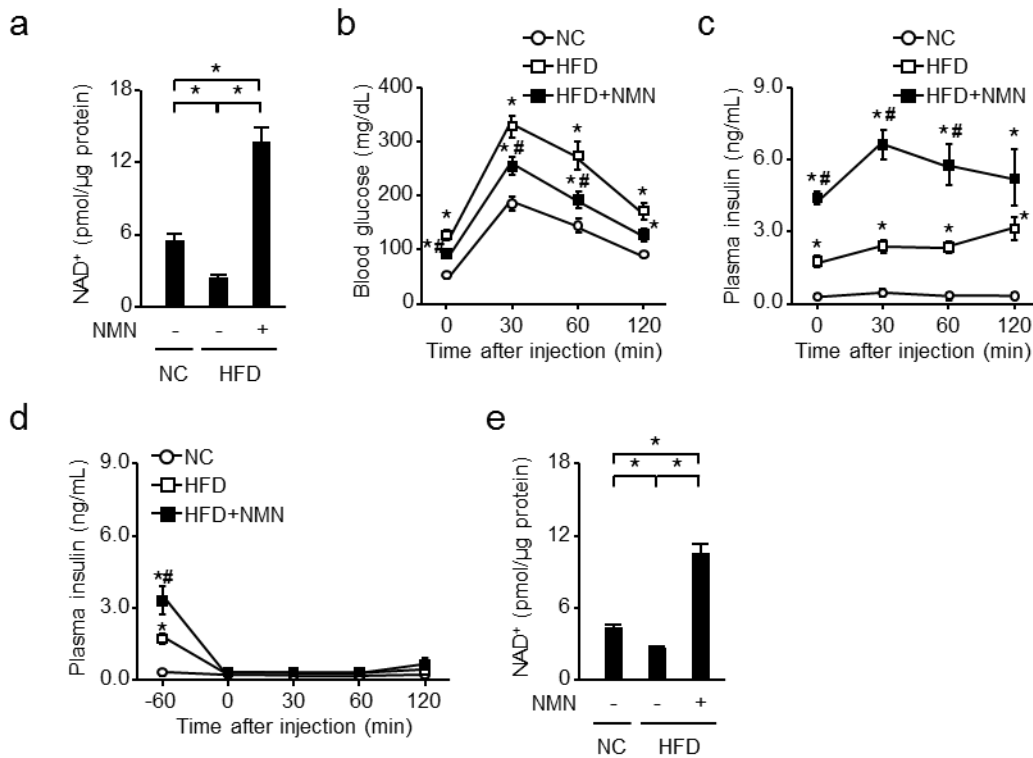
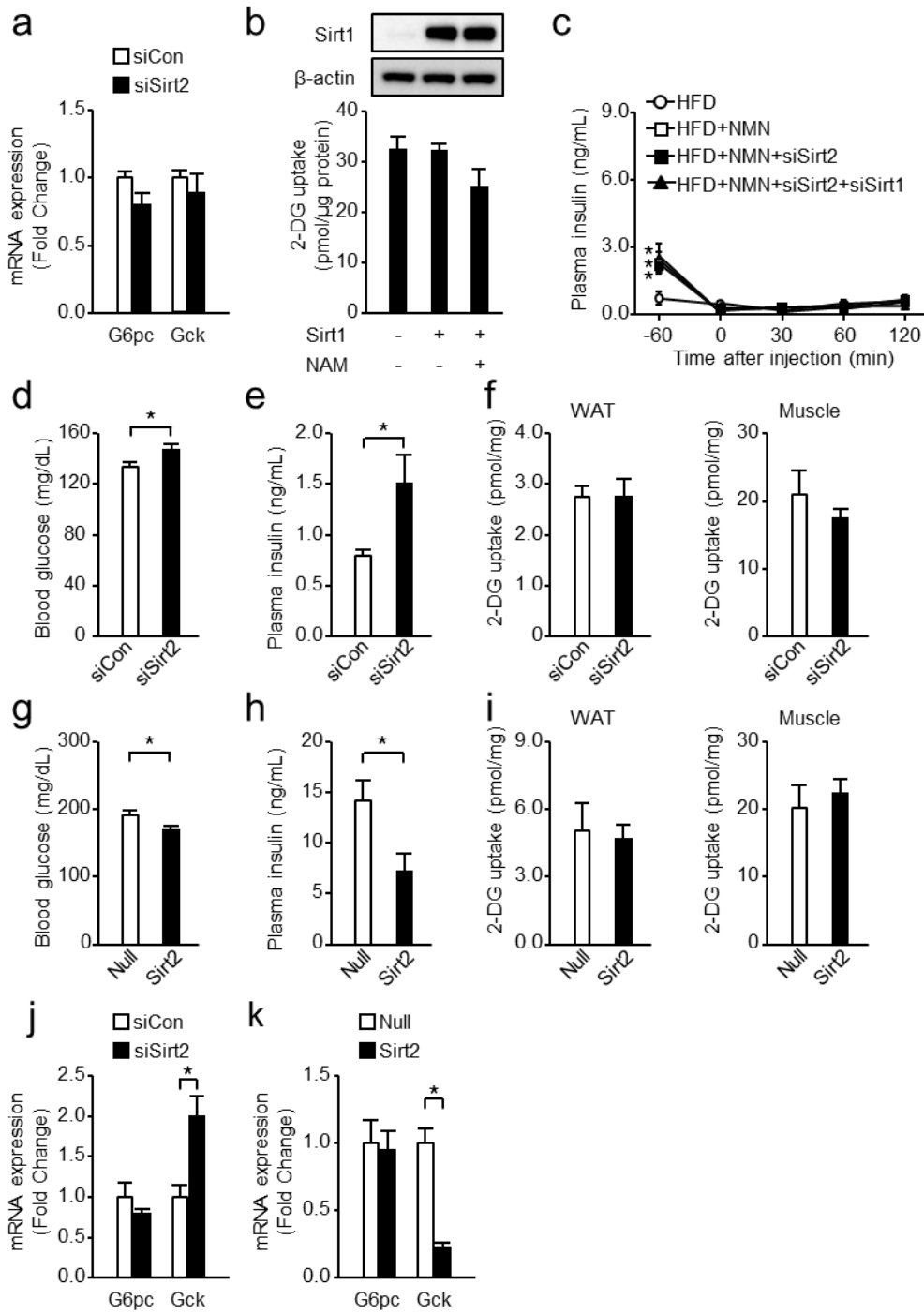


**Supplementary Figure 1. NAD<sup>+</sup> and hepatic expression of Gck and G6pc.** (a) Oil red O staining in primary hepatocytes derived from lean and db/db mice. Scale bars indicate 20  $\mu$ m. (b) Expressions of G6pc and Gck mRNA in primary hepatocytes derived from lean and db/db mice ( $n = 3$ ). (c) Effect of siRNA-mediated knockdown of Nampt and nicotinamide mononucleotide (NMN) on mRNA expressions of G6pc, Gck, and Nampt in mouse primary hepatocytes ( $n = 3$ ). (d) Effect of gallotannin (GTN) and NMN on mRNA expressions of G6pc and Gck in mouse primary hepatocytes ( $n = 3$ ). \* $P < 0.05$ ; one-way analysis of variance (ANOVA) with the Fisher's PLSD *post hoc* test (b–d). Error bars show the standard error of the mean (s.e.m).

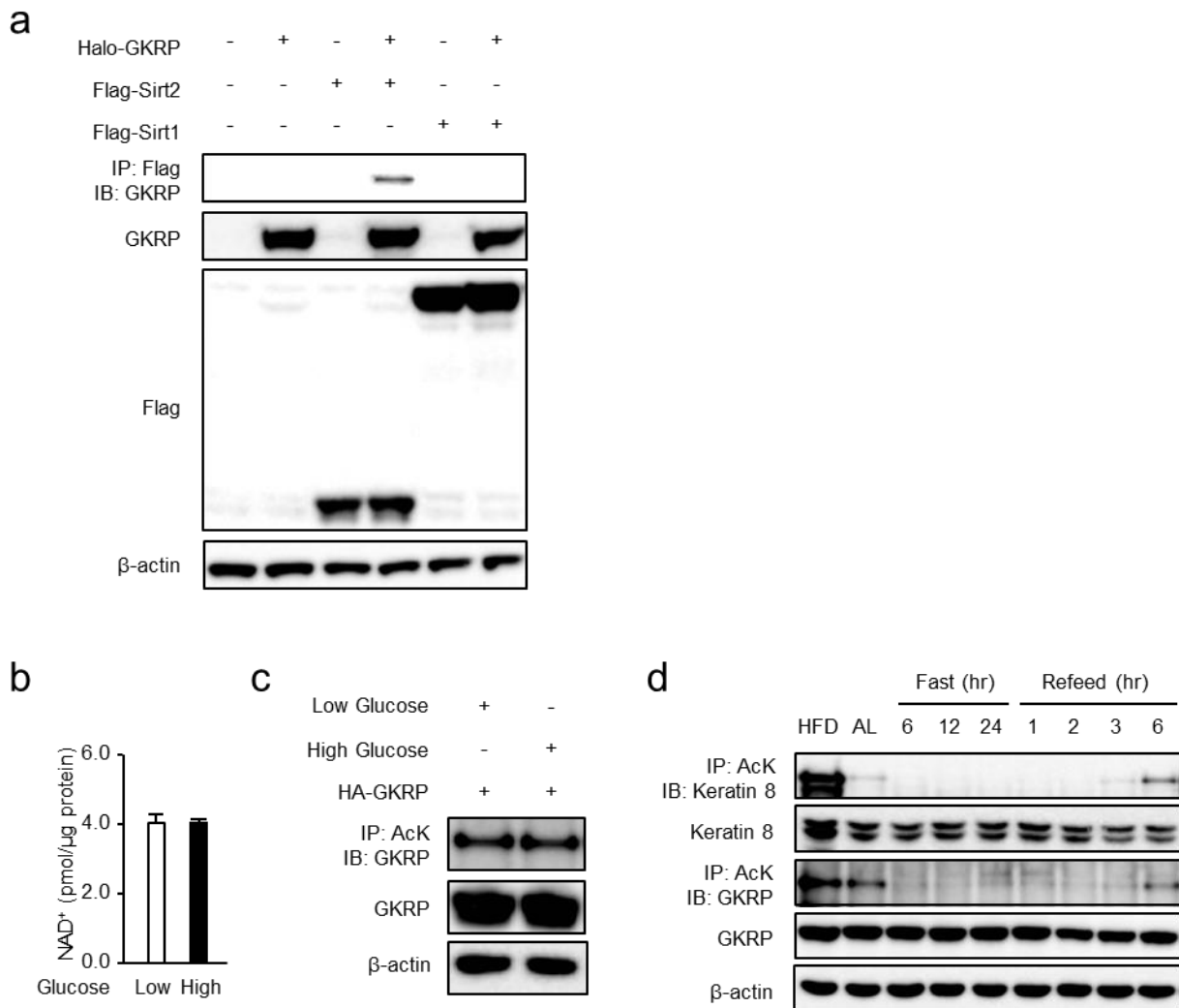


**Supplementary Figure 2. Glucose tolerance testing with and without NMN administration.** (a–c) NAD<sup>+</sup> level ( $n = 3$ ) (a) in the liver and blood glucose ( $n = 5$ ) (b) and plasma insulin (c) ( $n = 5$ ) levels in mice fed a normal chow diet (NC), high-fat diet (HFD), and a HFD and treated intraperitoneally with NMN after glucose loading (1 g/kg). (d,e) Plasma insulin level ( $n = 5$ ) (d) and NAD<sup>+</sup> level in the liver (e) ( $n = 3$ ) in NC, HFD, and HFD mice treated with NMN after glucose administration (1 g/kg) with concomitant continuous dosing of somatostatin (3 μg/kg/min). \* $P < 0.05$ ; one-way ANOVA with the Fisher's PLSD *post hoc* test (a,e), \* $P < 0.05$ , versus NC; # $P < 0.05$ , HFD versus HFD with NMN in b–d; one-way ANOVA with the Fisher's PLSD *post hoc* test. Error bars show s.e.m.



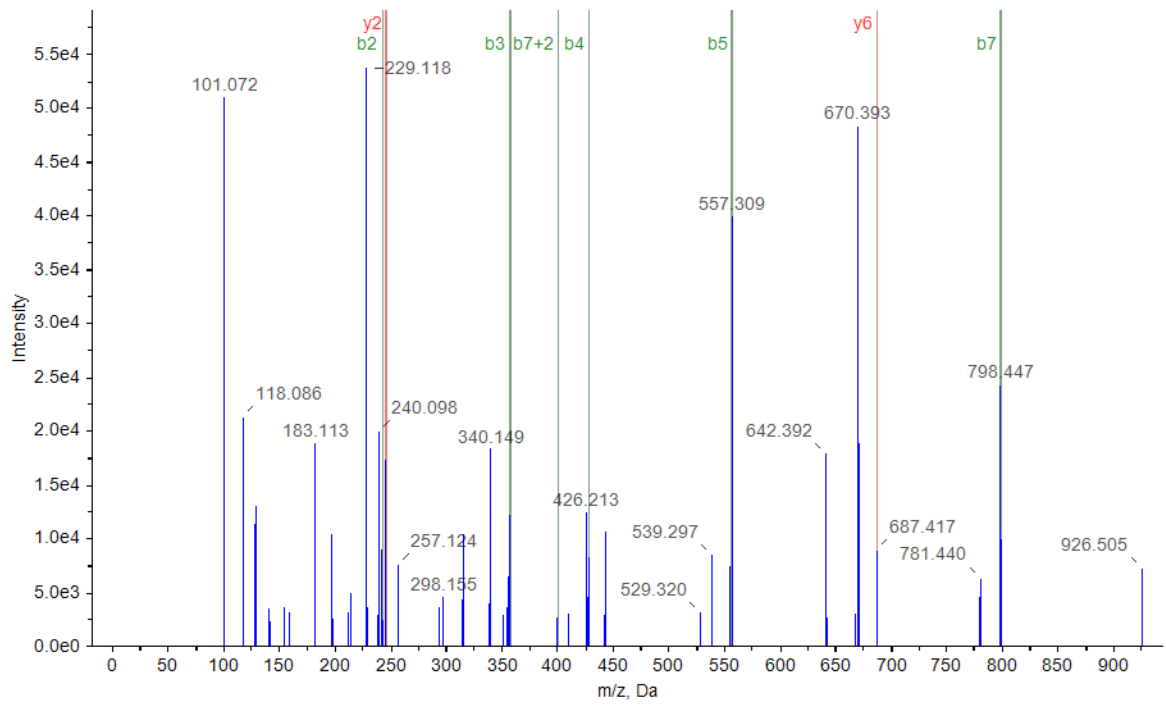
**Supplementary Figure 3. Phenotypes of mice with hepatic Sirt2 knockdown or overexpression.**

(a) Gene expression of G6pc and Gck in mouse primary hepatocytes treated with or without siSirt2 ( $n = 3$ ). (b) Effect of adenovirus-mediated overexpression of Sirt1 on 2-DG uptake in primary hepatocytes derived from db/db mouse in the presence or absence of NAM ( $n = 4$ ). (c) Plasma insulin level during glucose tolerance testing (1 g/kg) in HFD mice treated with NMN in the presence or absence of hepatic Sirt2 knockdown or Sirt2 and Sirt1 double knockdown during continuous dosing of somatostatin ( $n = 5$ ). (d,e) Blood glucose (d) and plasma insulin (e) levels of hepatic Sirt2 knockdown lean mice under free-feeding conditions ( $n = 9$ ). (f) Uptake of 2-deoxyglucose in the white adipose tissue (WAT) and skeletal muscle of hepatic Sirt2 knockdown lean mice after glucose administration (2 g/kg) ( $n = 4$ ). (g,h) Levels of blood glucose (g) and plasma insulin (h) of HFD-fed mice with adenovirus-mediated hepatic Sirt2 overexpression under free-feeding conditions ( $n = 7$ ). (i) Uptake of 2-deoxyglucose in the WAT and skeletal muscle in hepatic Sirt2-overexpressing lean mice after glucose administration (1 g/kg) ( $n = 5$ ). (j,k) Hepatic mRNA expression of G6pc and Gck in hepatic Sirt2 knockdown mice ( $n = 4$ ) (j) and in HFD-fed mice with adenovirus-mediated hepatic Sirt2 overexpression ( $n = 5$ ) (k). \* $P < 0.05$ ; Student's *t*-test (a,d–k) and one-way ANOVA with the Fisher's PLSD *post hoc* test (b). \* $P < 0.05$ , versus HFD in c; one-way ANOVA with the Fisher's PLSD *post hoc* test. Error bars show s.e.m.

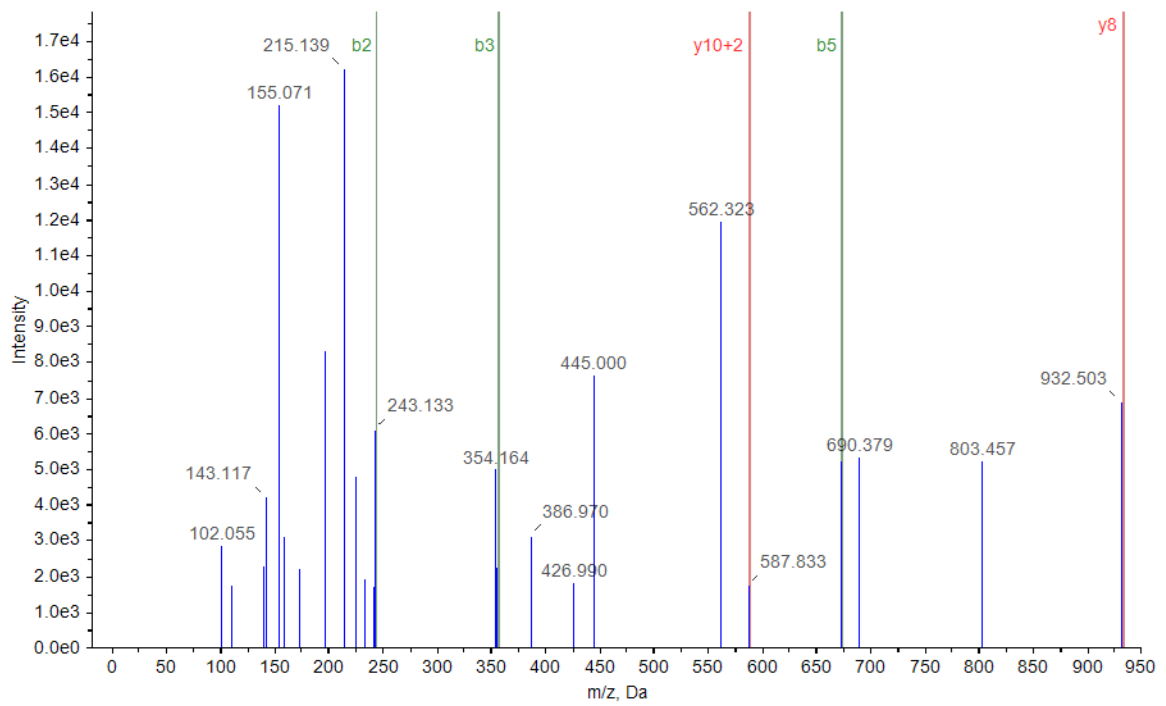


**Supplementary Figure 4. Acetylated GKRP levels in hepatocytes cultured under low- or high-glucose conditions and in the liver under fasted/refed conditions.** (a) Immunoprecipitation and immunoblot analysis of the interaction between Sirt2 and GKRP or Sirt1 and GKRP in HEK293 cells expressing Flag-tagged Sirt2, Flag-tagged Sirt1, or Halo-tagged GKRP. (b) NAD<sup>+</sup> level in mouse primary hepatocytes cultured in low- or high-glucose medium ( $n = 5$ ). (c) Acetylation level of GKRP in mouse primary hepatocytes cultured in low- or high-glucose medium. (d) Successive comparison of lysine acetylation levels of keratin 8 and GKRP in the liver of NC-fed mice under a fasted/refed condition for the indicated times, and under ad libitum-fed conditions (AL). Error bars show s.e.m.

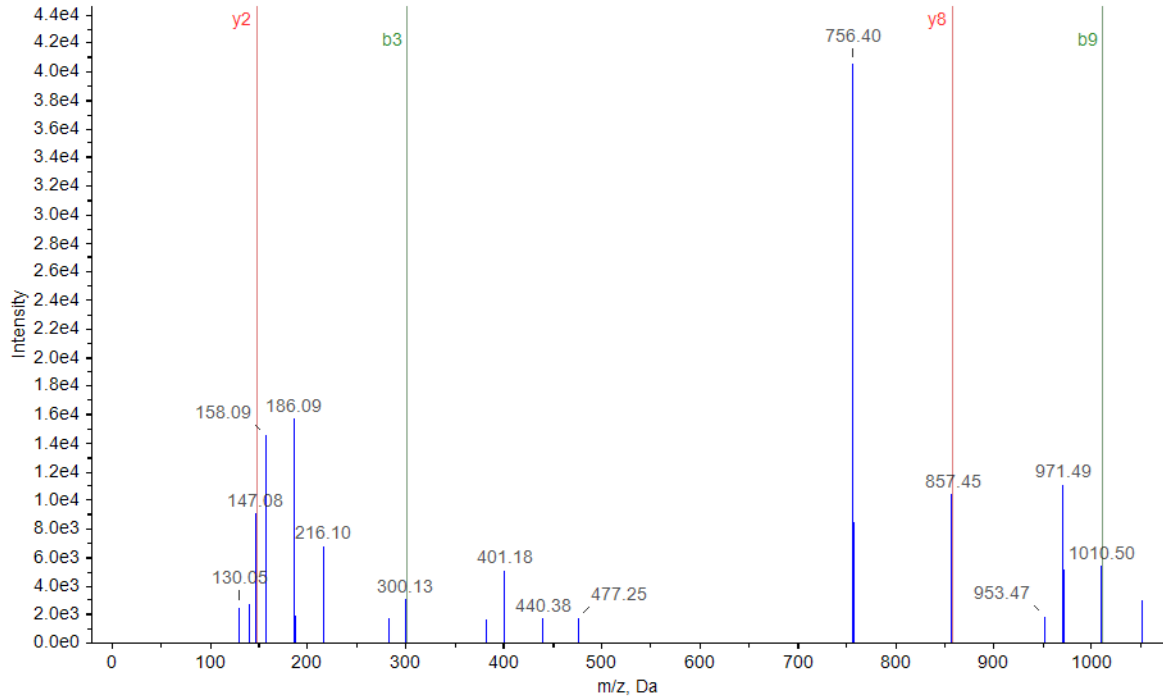
**a** K43: K\*ADAEKIVQ



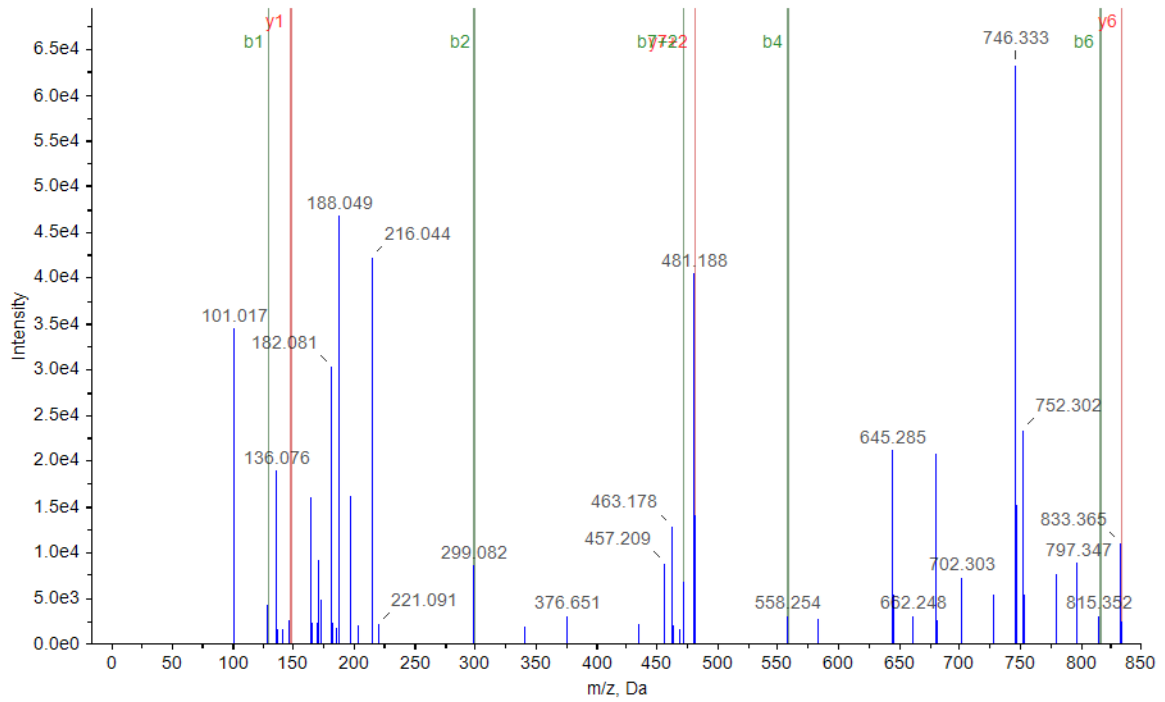
**b** K126: NQLMK\*GLGQK



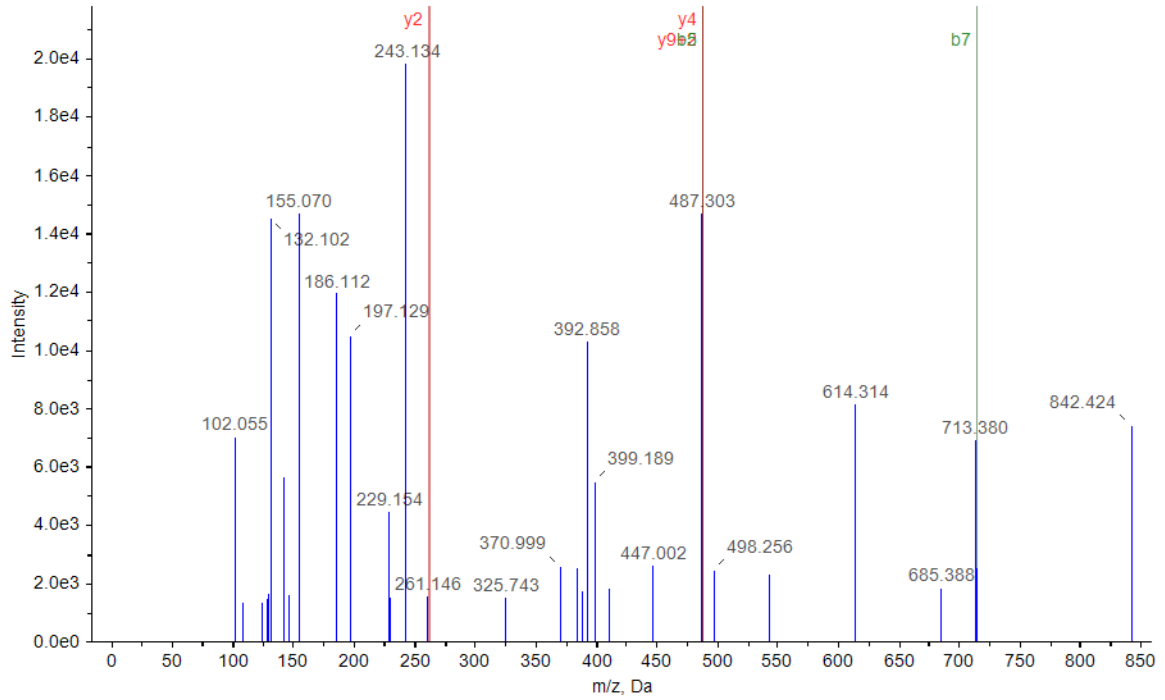
**c** K165: GIEELKK\*VAAG



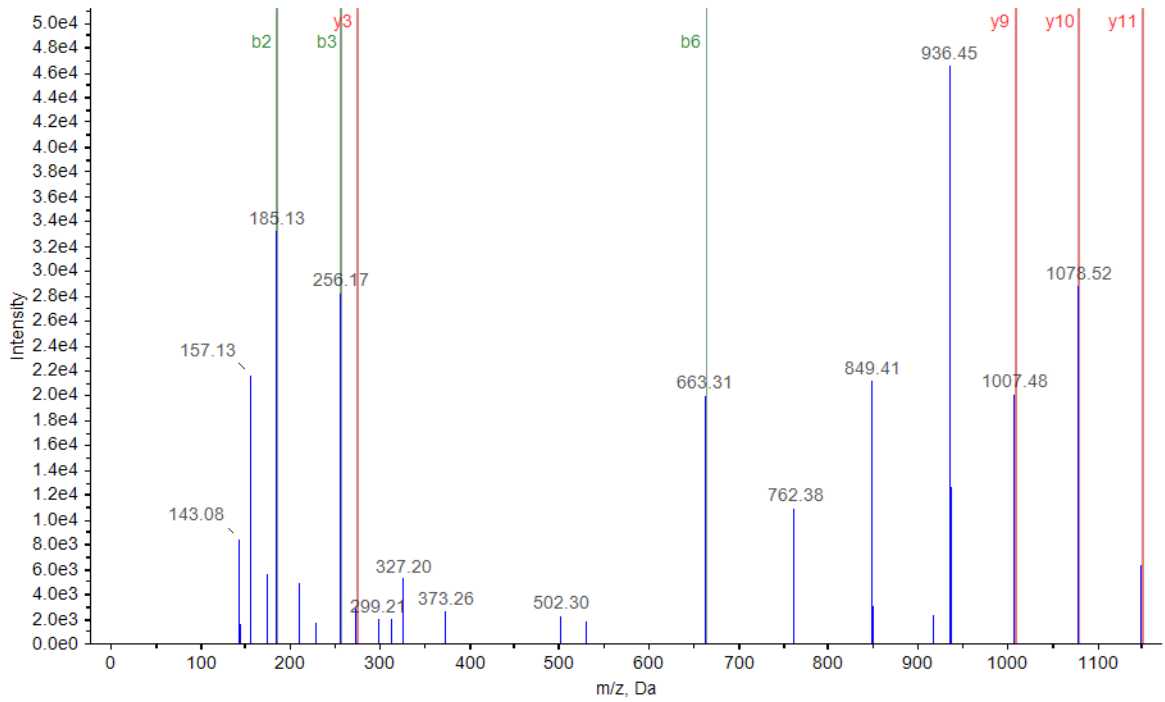
**d** K235: QK\*MQEKQ



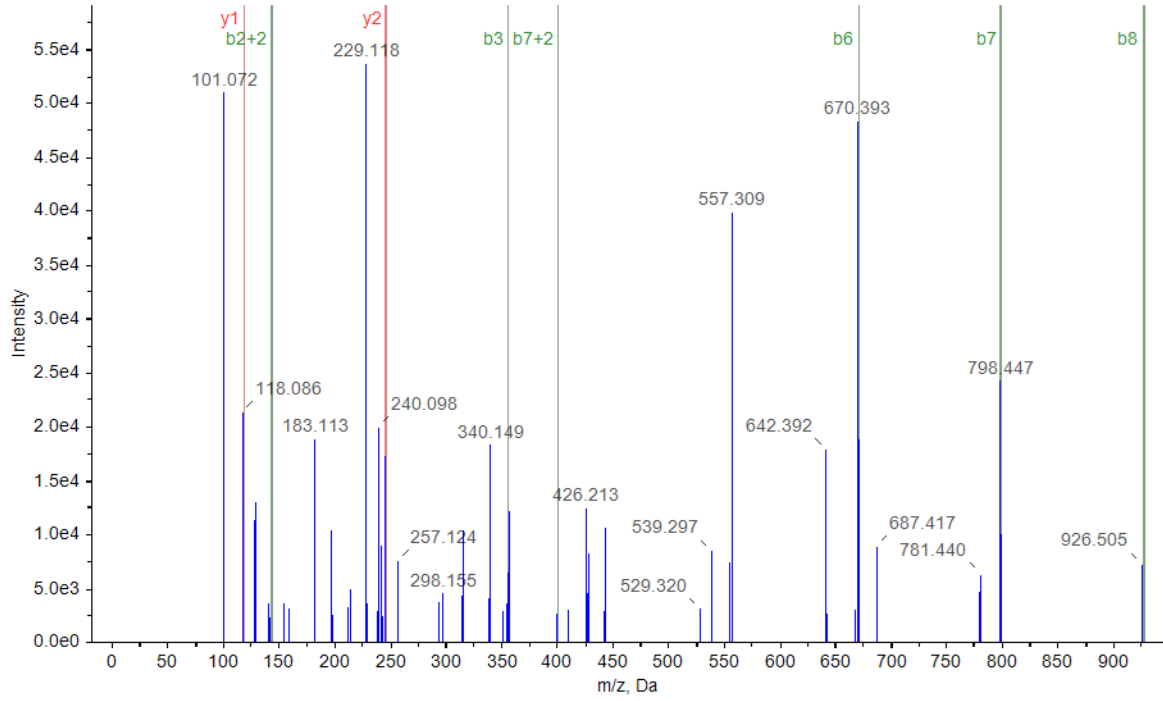
e K267: GSATK\*ILLE



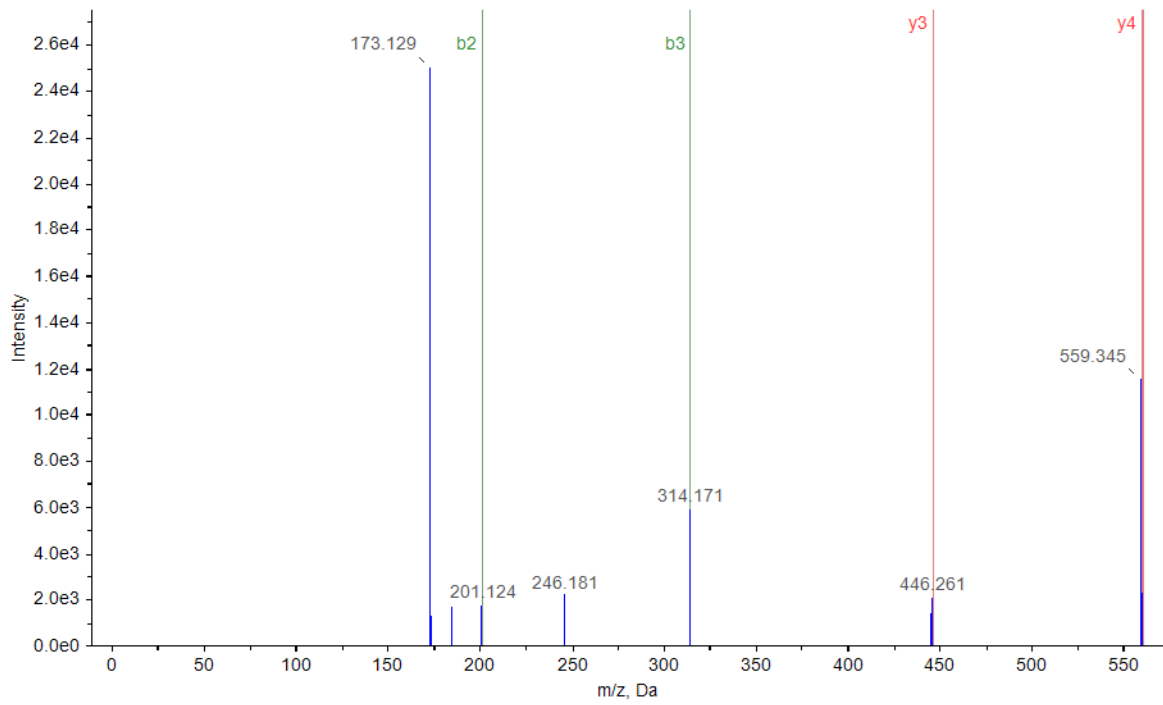
f K279: LAAHK\*TVDQGVV



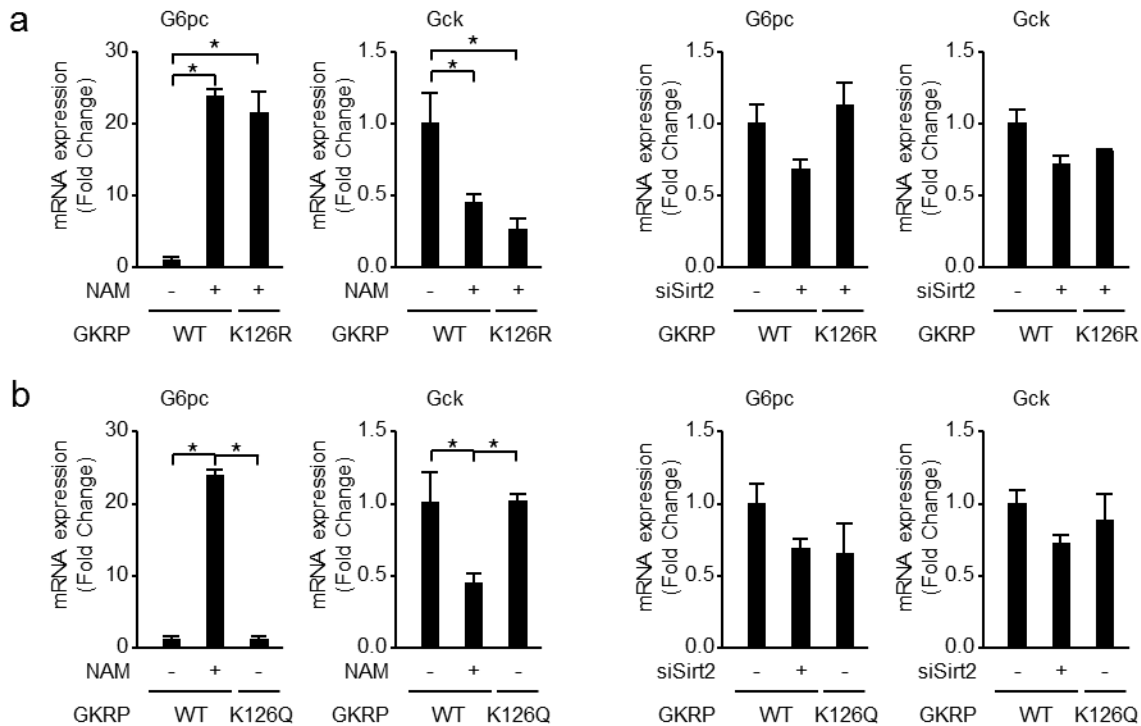
g K312: K\*IATLTKQV



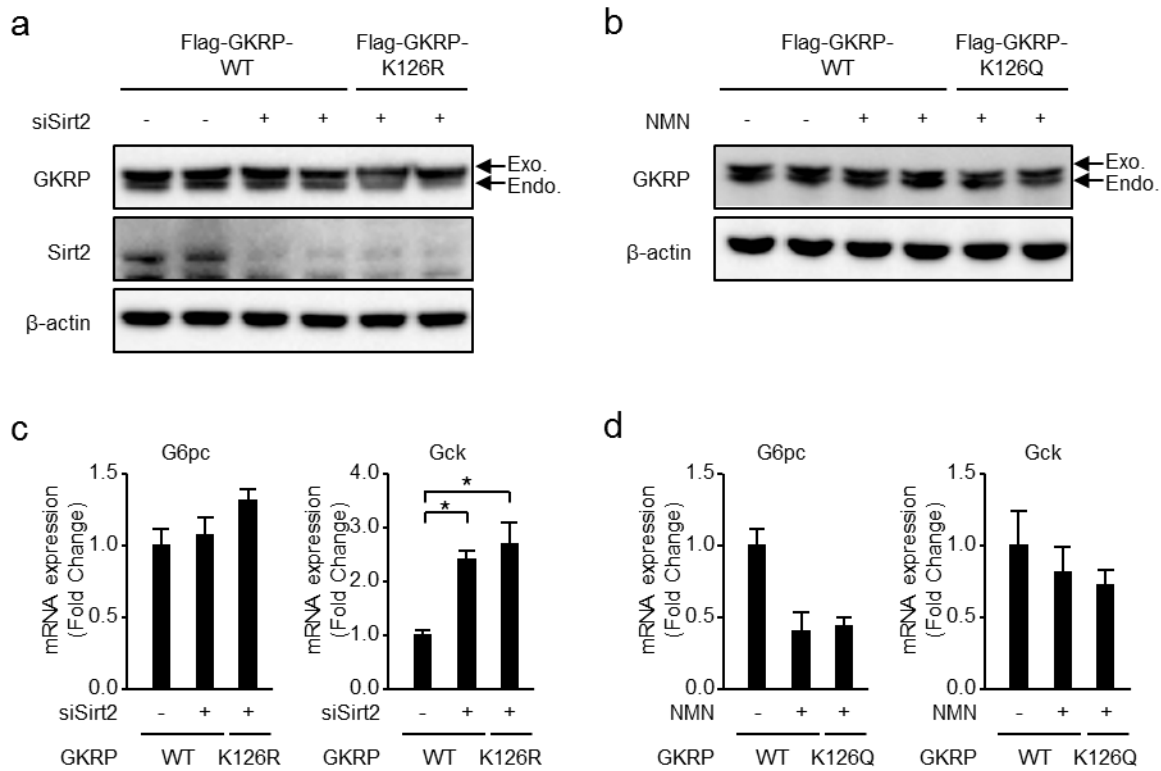
h K327: ISLEKK\*



**Supplementary Figure 5. Mass spectrometry analysis to determine the acetylation site of GKRP. (a–h)** Detection of acetylated lysines 43, 126, 235, 267, 279, 312, and 327 in mouse GKRP by MS/MS analysis. MS/MS spectra of the GKRP-derived peptides are shown, with the C-terminal y ions and N-terminal b ions labelled as assigned. K\*, acetylated lysine.

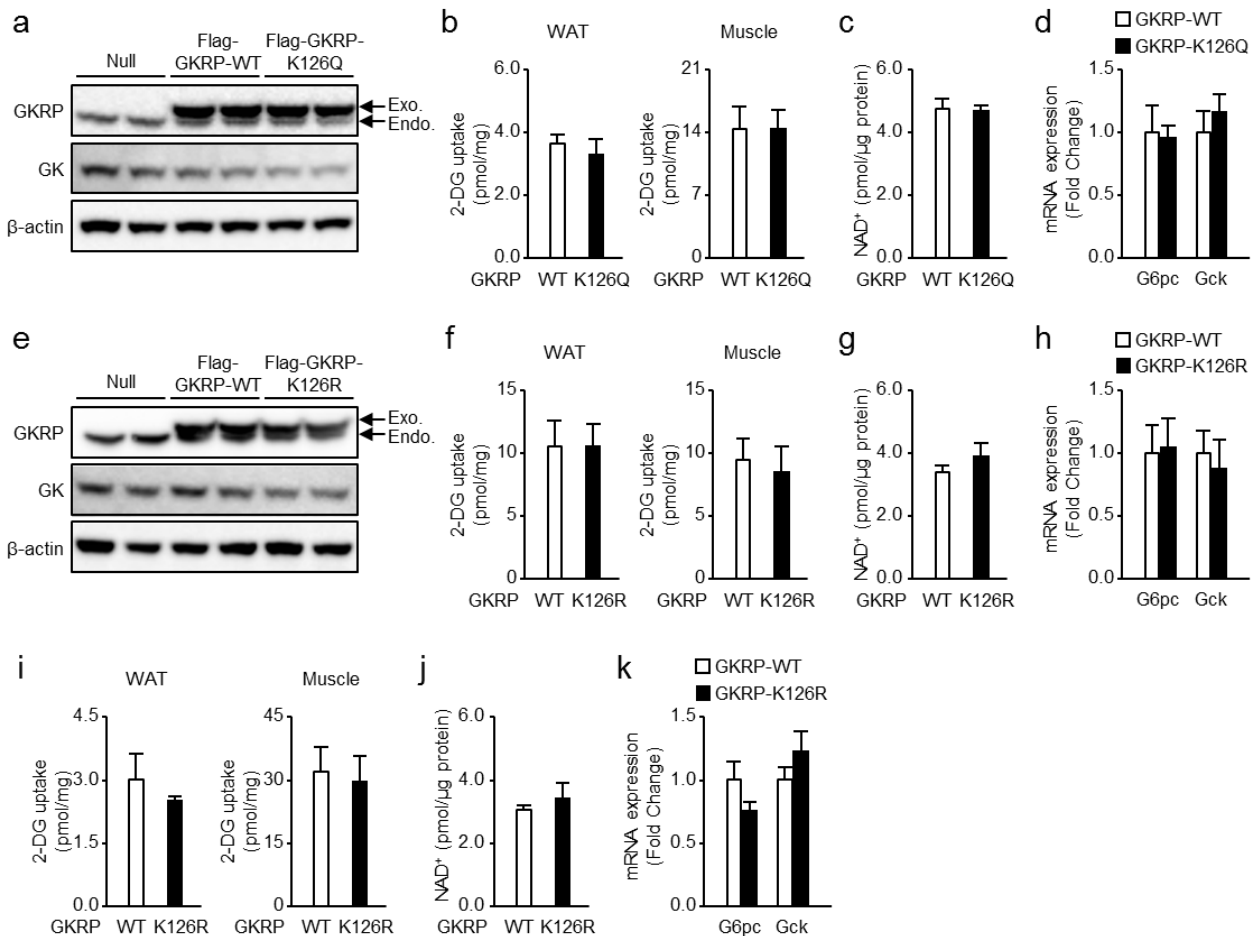


**Supplementary Figure 6. GKRP-K126R or K126Q mutant has no effect on *Gck* and *G6pc* mRNA expression in primary hepatocytes.** (a) Gene expression of *G6pc* and *Gck* in mouse primary hepatocytes transfected with adenovirus encoding Flag-tagged GKRP-wild-type (GKRP-WT) and Flag-tagged GKRP-K126R with NAM treatment or Sirt2 knockdown ( $n = 4$ ). (b) Gene expression of *G6pc* and *Gck* in mouse primary hepatocytes transfected with adenovirus encoding Flag-tagged GKRP-WT and Flag-tagged GKRP-K126Q with NAM treatment or Sirt2 knockdown ( $n = 4$ ).  $*P < 0.05$ ; one-way ANOVA with the Fisher's PLSD *post hoc* test (a,b). Error bars show s.e.m.



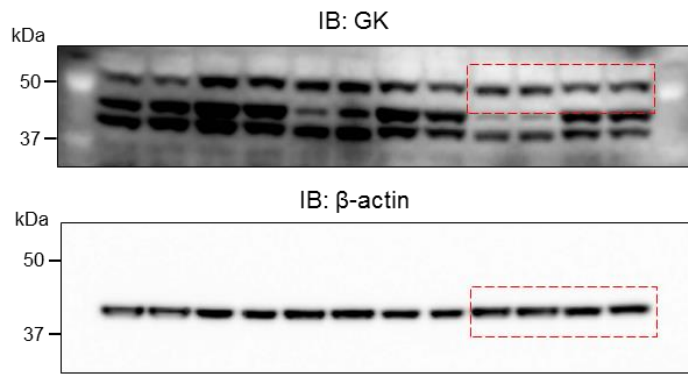
**Supplementary Figure 7. GKR-K126R or K126Q mutant has no effect on hepatic *Gck* and *G6pc* mRNA expression in mice.** (a,b) Hepatic GKRP protein expression in Sirt2 knockdown mice transfected with an adenovirus for Flag-tagged GKRP- WT and Flag-tagged GKRP-K126R (a) and in NMN-treated HFD-fed mice transfected with an adenovirus for Flag-tagged GKRP-WT and Flag-tagged GKRP-K126Q (b). Endo., endogenous GKRP; Exo., exogenous GKRP. (c,d) Hepatic *G6pc* and *Gck* mRNA expression in Sirt2 knockdown mice transfected with an adenovirus for Flag-tagged GKRP- WT and Flag-tagged GKRP-K126R (c) and in NMN-treated HFD-fed mice transfected with an adenovirus for Flag-tagged GKRP-WT and Flag-tagged GKRP-K126Q (d) ( $n = 4$ ).  $*P < 0.05$ ; one-way ANOVA with the Fisher's PLSD *post hoc* test (c,d). Error bars show s.e.m.

Supplementary Figure 8

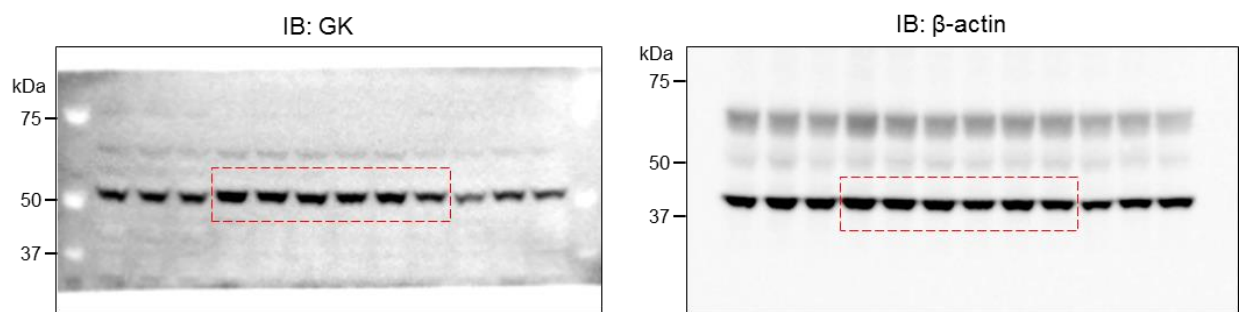


**Supplementary Figure 8. GKRK-K126R or K126Q mutant has no effect on 2-DG uptake in the WAT and skeletal muscle and the gene expression of glucokinase and glucose-6-phosphatase in the liver.** (a) Immunoblot analysis of GKRK in the liver of lean mice transfected with an adenovirus for Flag-tagged GKRK-WT or Flag-tagged GKRK-K126Q. Endo., endogenous GKRK; Exo., exogenous GKRK. (b–d) Uptake of 2-deoxyglucose (2-DG) in the white adipose tissue (WAT) and skeletal muscle ( $n = 5$ ) (b), hepatic NAD<sup>+</sup> levels ( $n = 4$ ) (c) and hepatic *G6pc* and *Gck* mRNA expression ( $n = 4$ ) (d) in mice with GKRK-WT or GKRK-K126Q overexpression. (e) Immunoblot analysis of GKRK in the liver of HFD mice transfected with an adenovirus for Flag-tagged GKRK-WT or Flag-tagged GKRK-K126R. (f–h) Uptake of 2-DG in the white adipose tissue (WAT) and skeletal muscle ( $n = 5$ ) (f), hepatic NAD<sup>+</sup> levels ( $n = 4$ ) (g), and hepatic *G6pc* and *Gck* mRNA expression ( $n = 4$ ) (h) in HFD mice with hepatic GKRK-WT or GKRK-K126R overexpression. (i–k) Uptake of 2-DG in the white adipose tissue (WAT) and skeletal muscle ( $n = 5$ ) (i), hepatic NAD<sup>+</sup> levels ( $n = 4$ ) (j) and hepatic *G6pc* and *Gck* mRNA expression ( $n = 4$ ) (k) in db/db mice with hepatic overexpression of Flag-tagged GKRK-WT or Flag-tagged GKRK-K126R. Error bars show s.e.m.

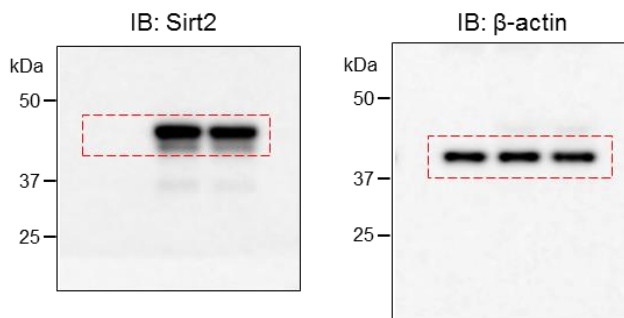
a



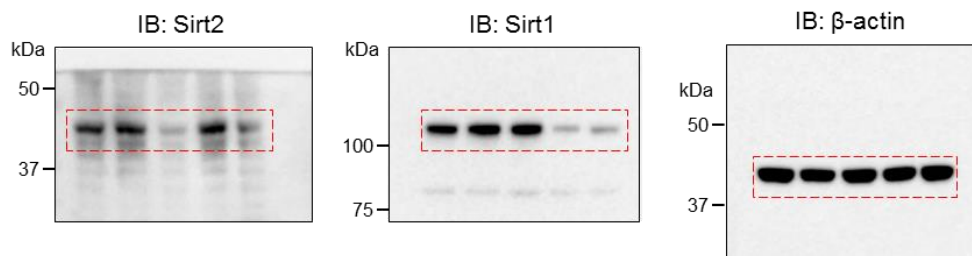
b



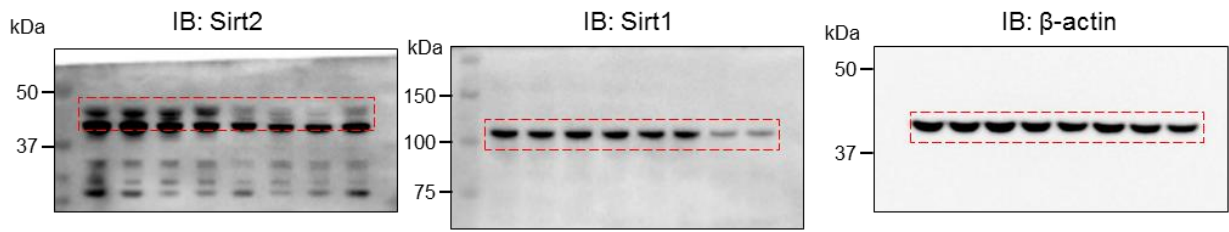
c



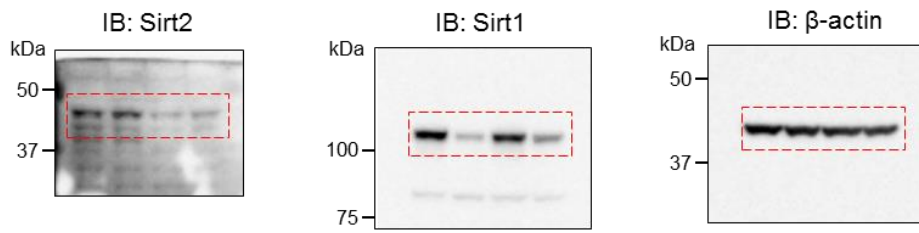
d



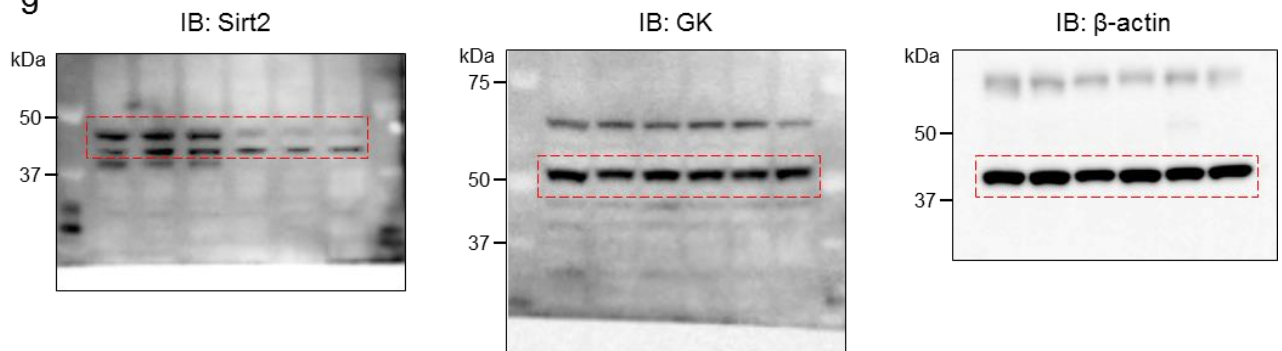
e



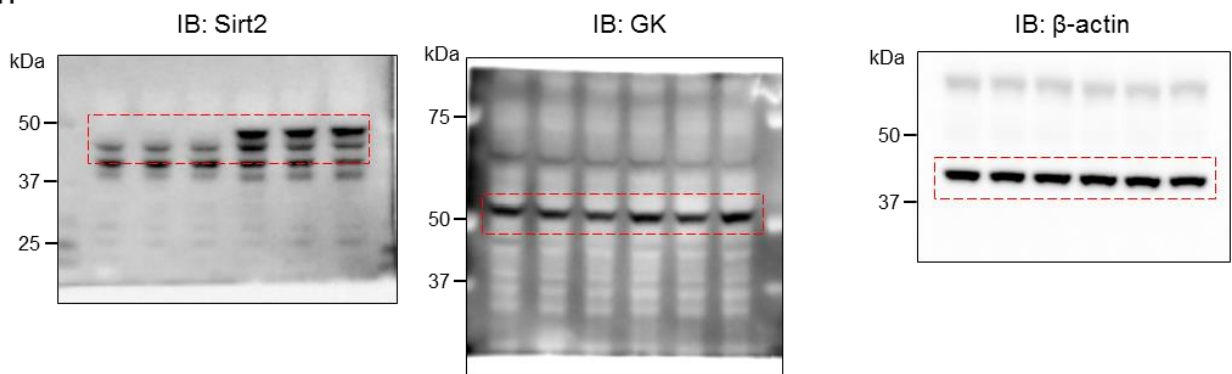
f



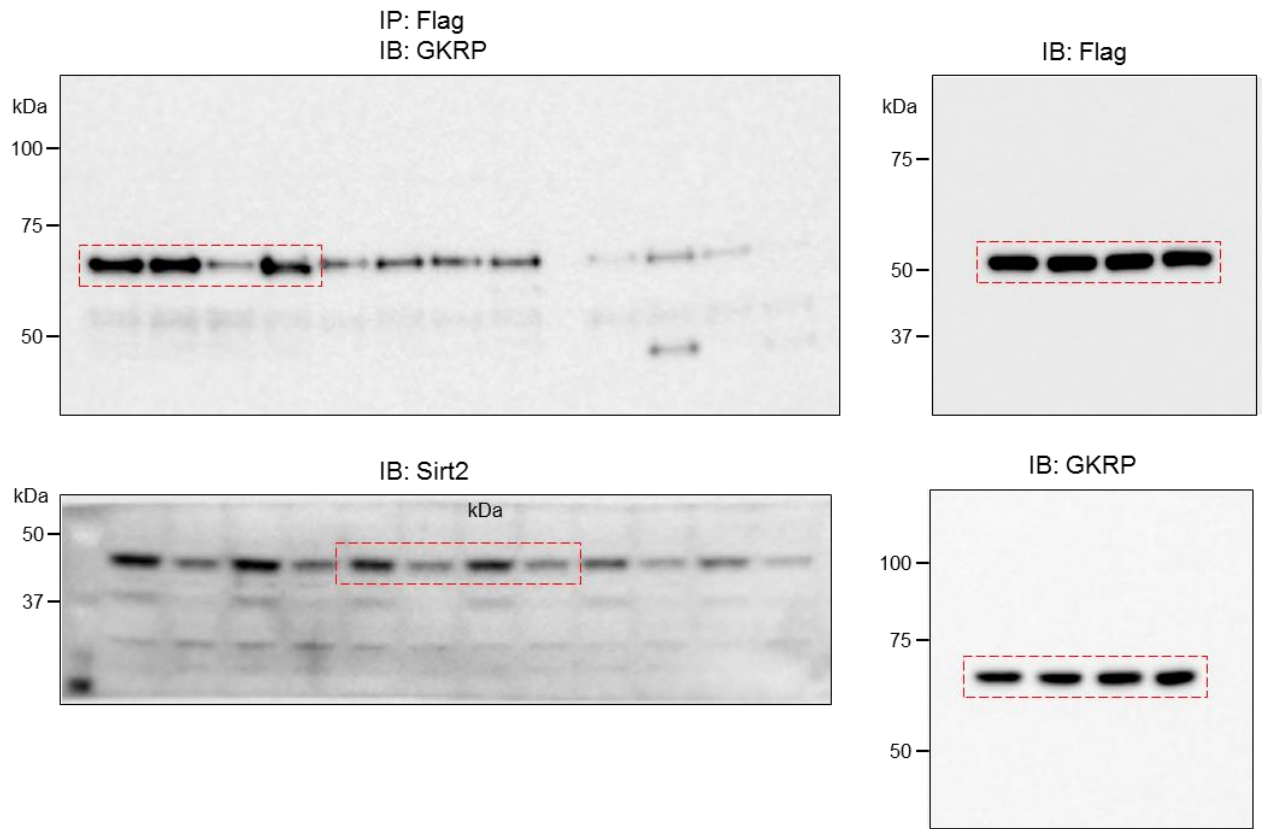
g



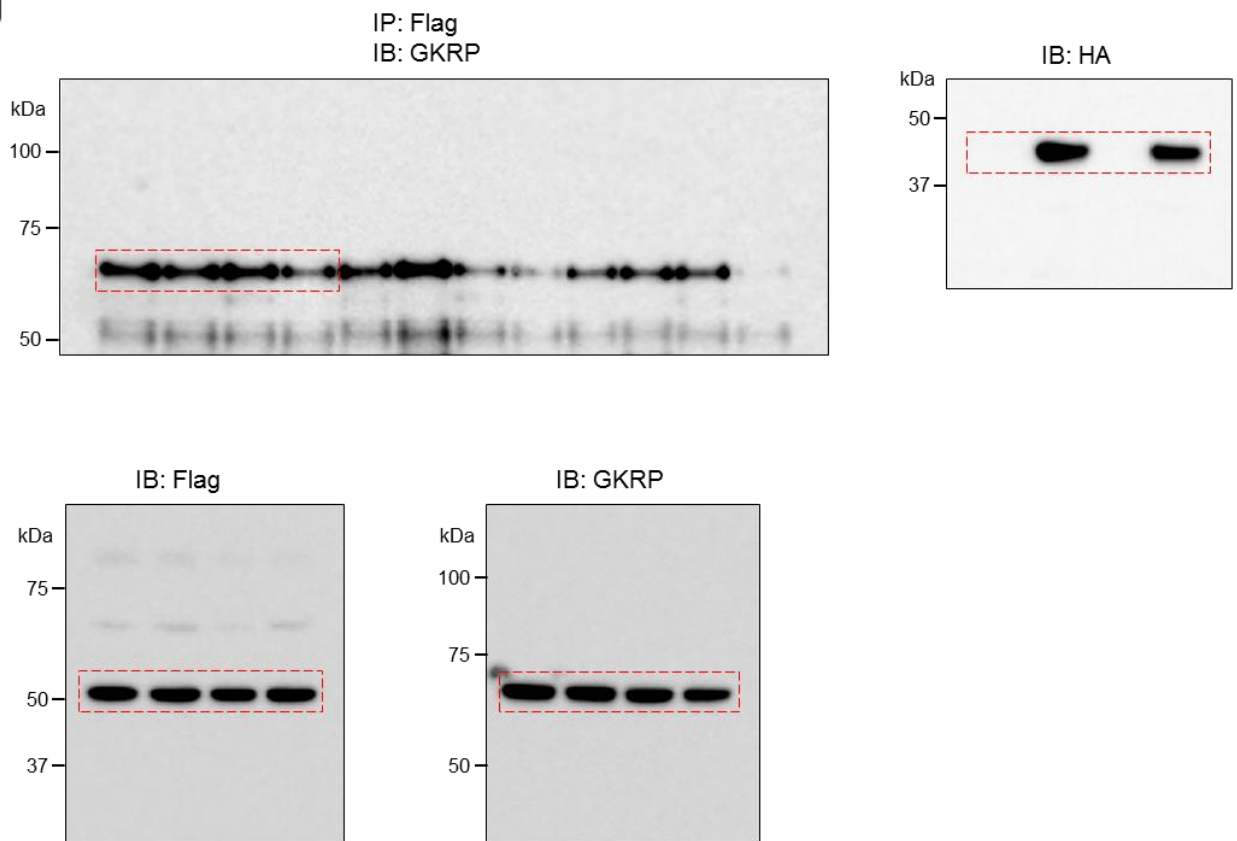
h



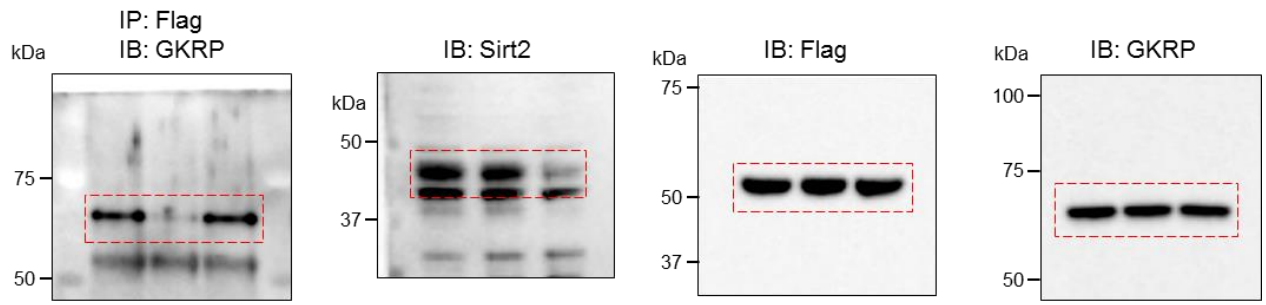
i



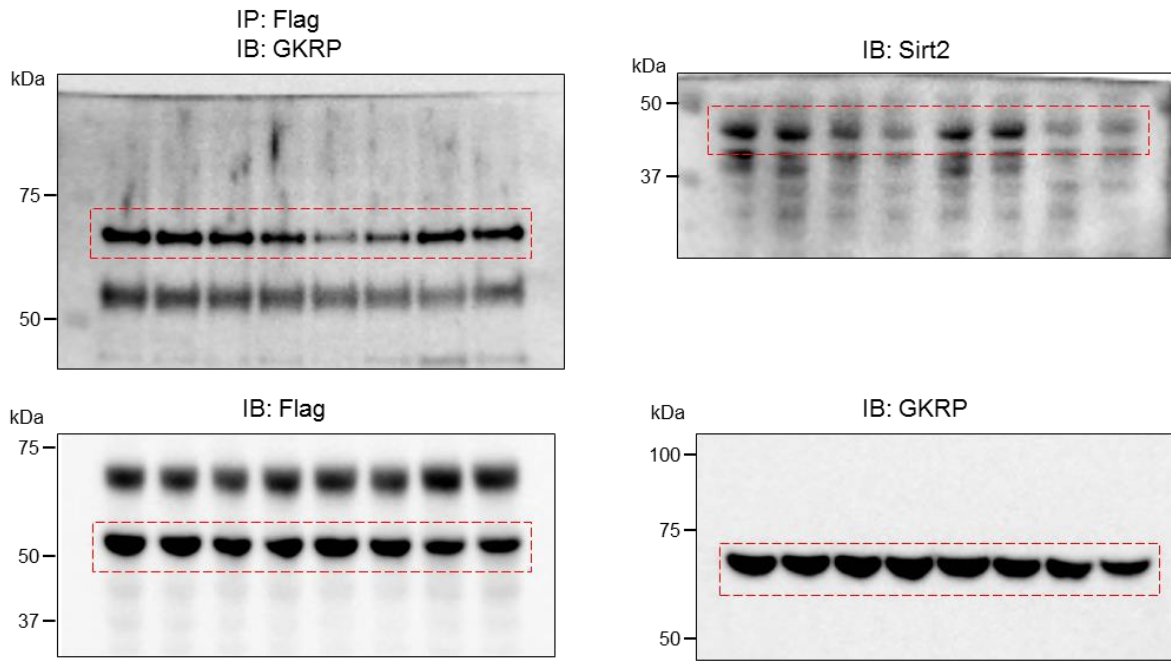
j



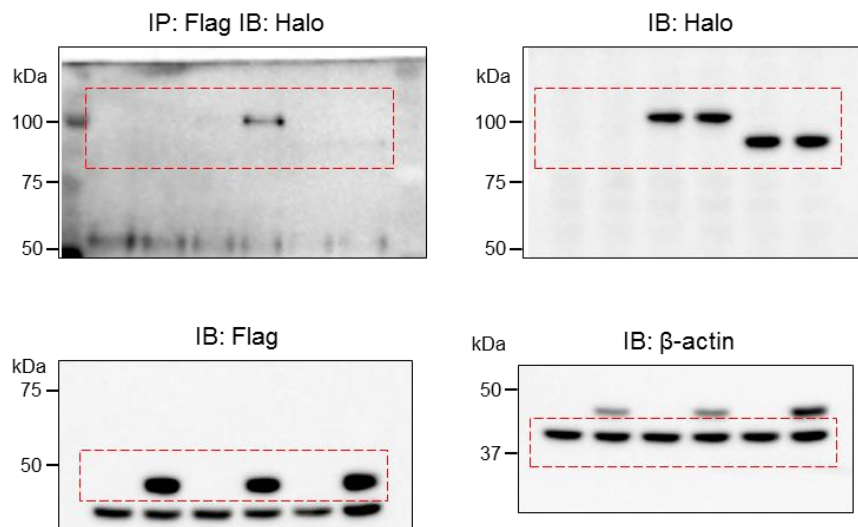
**k**



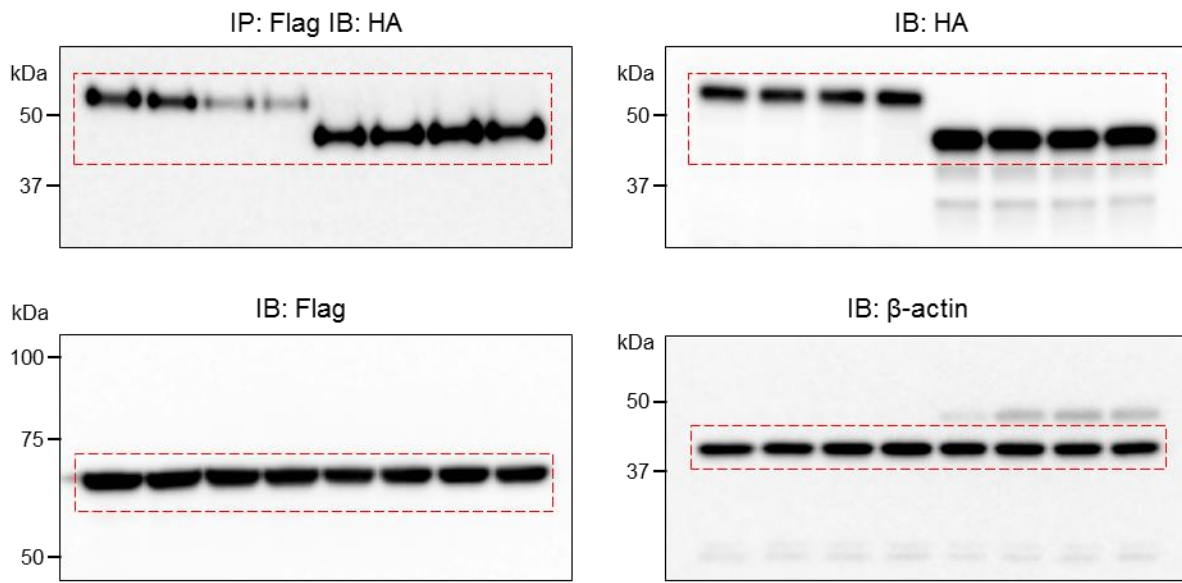
**l**



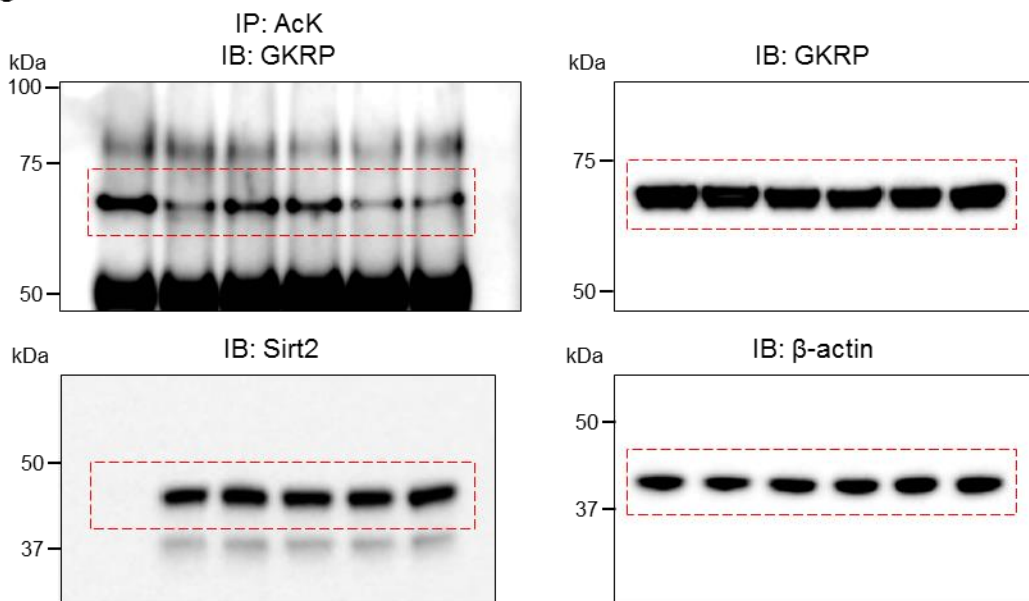
**m**



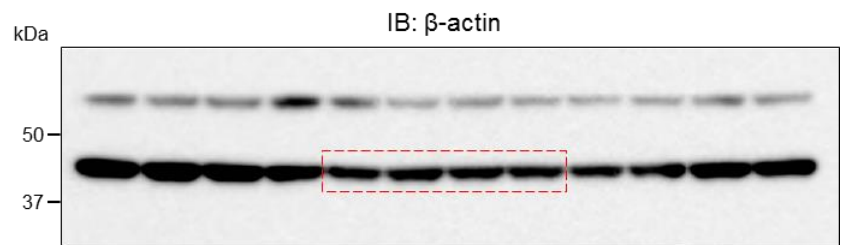
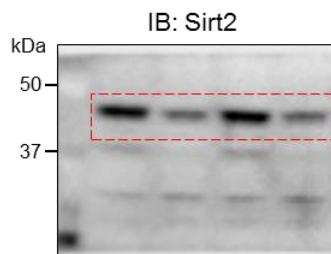
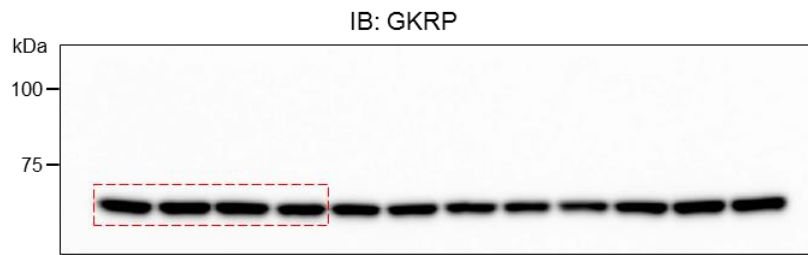
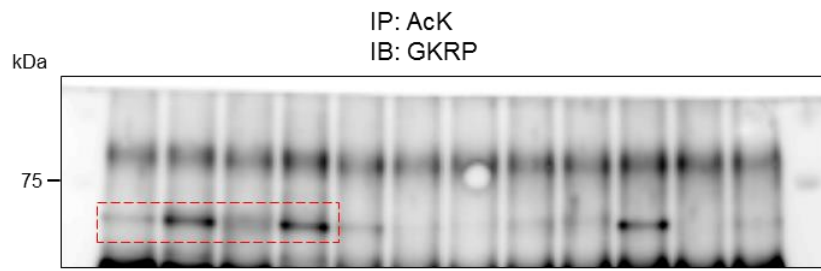
n



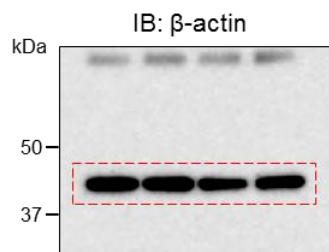
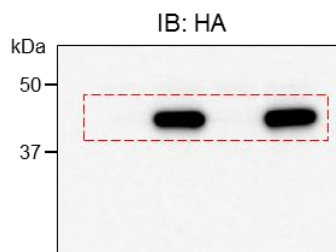
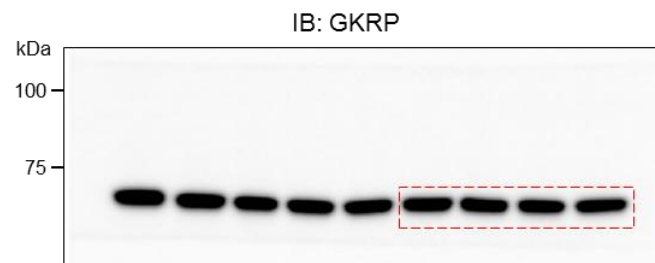
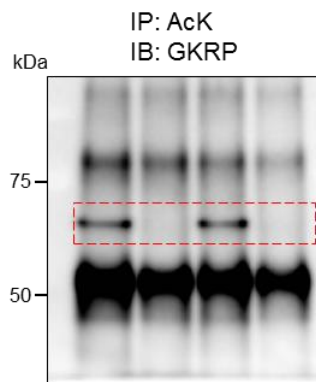
O



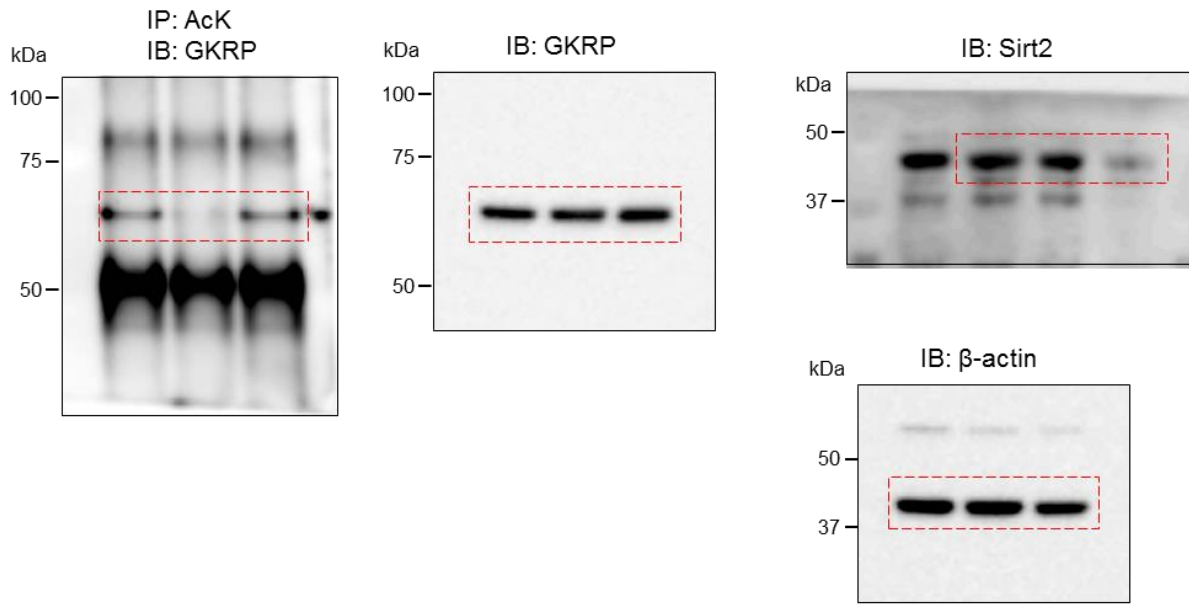
p



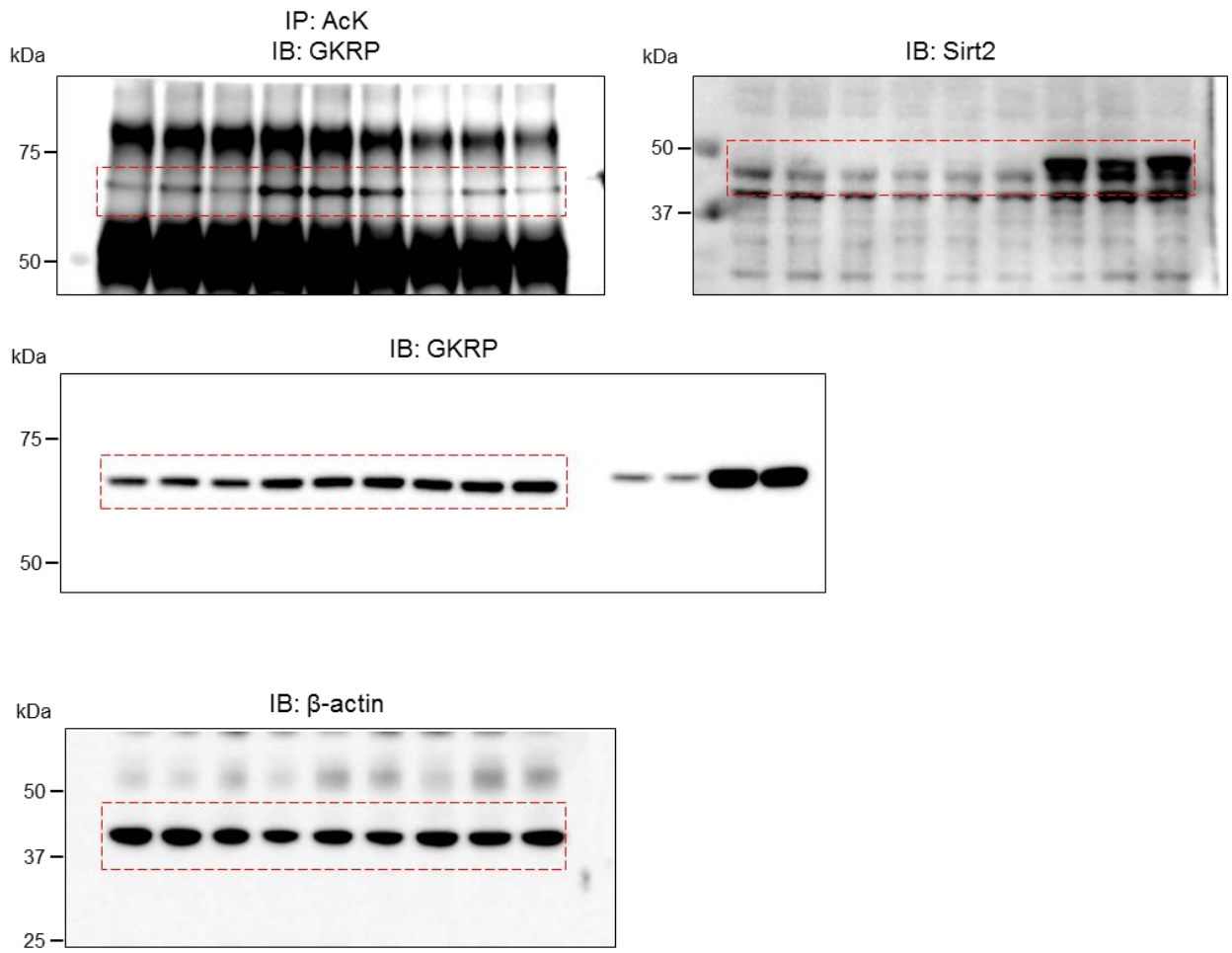
q



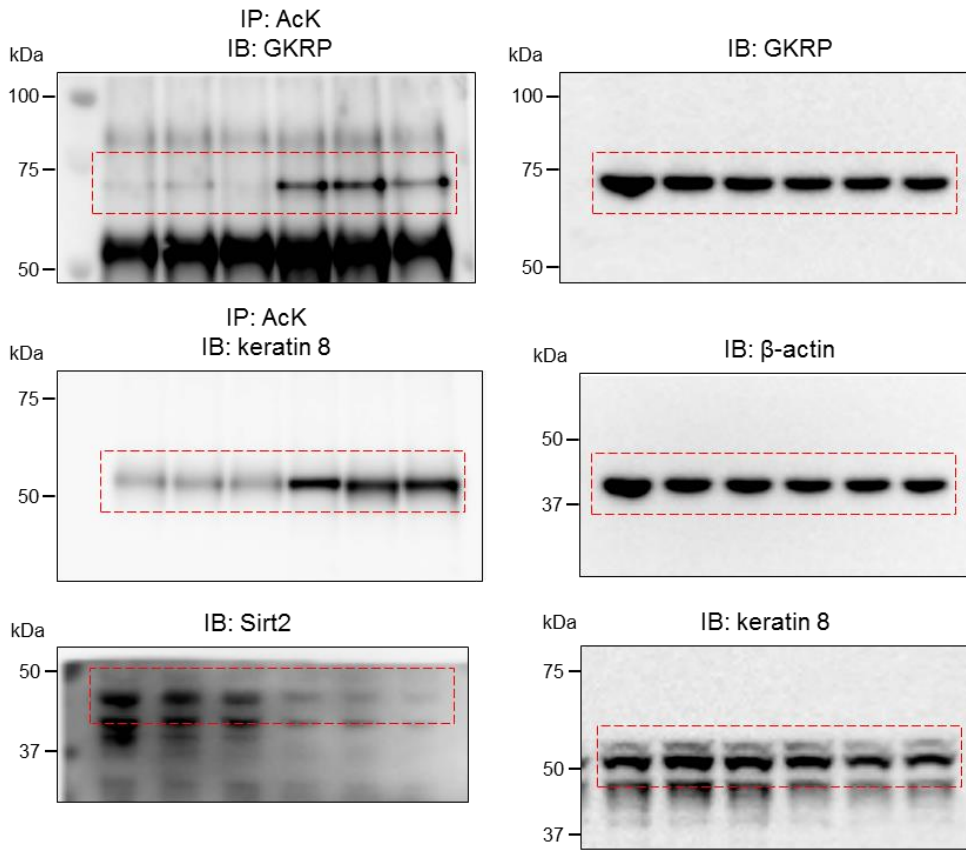
r



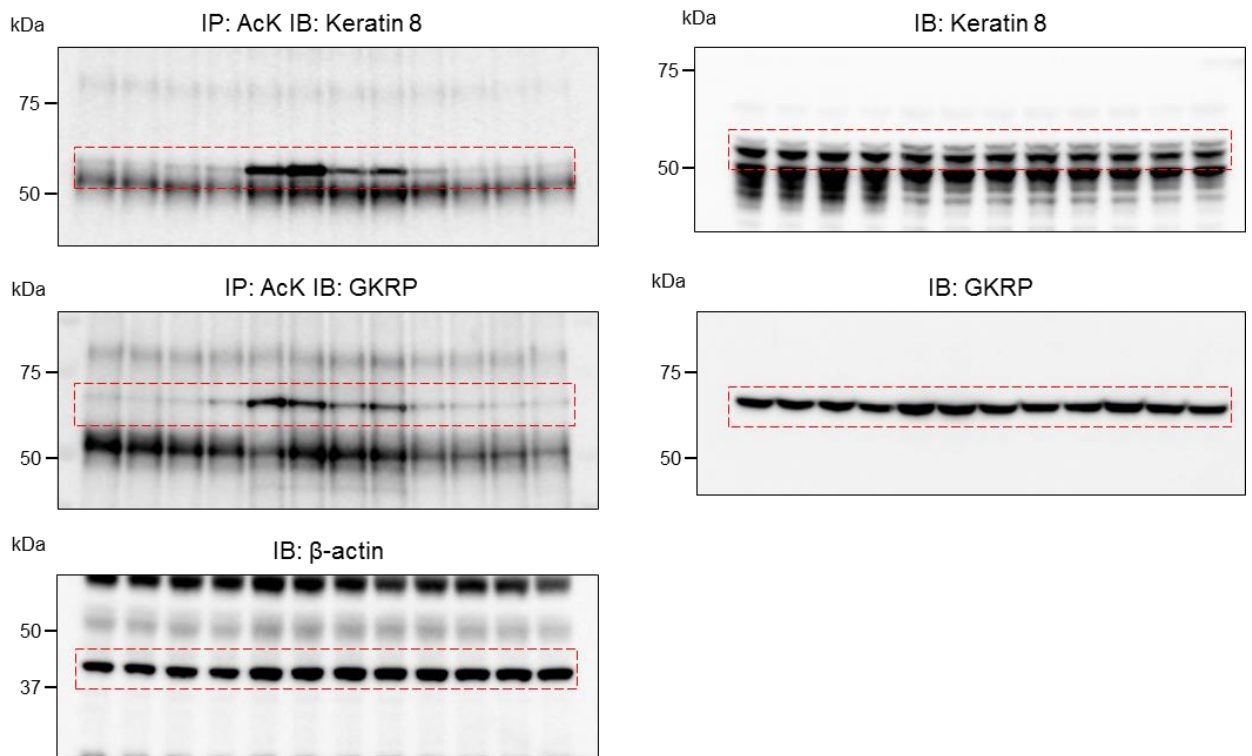
S



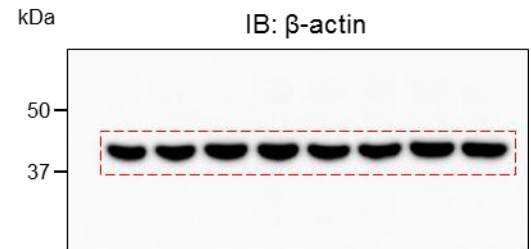
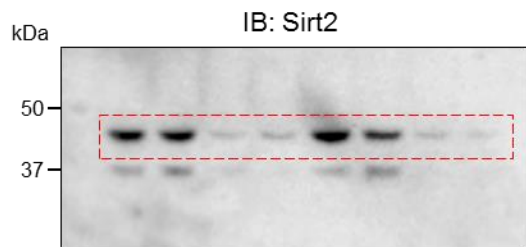
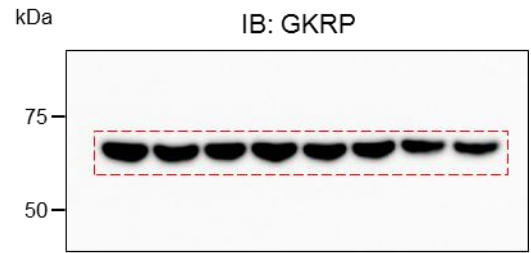
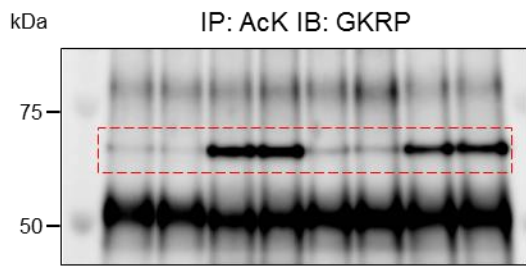
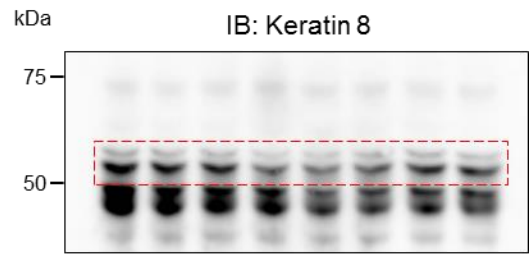
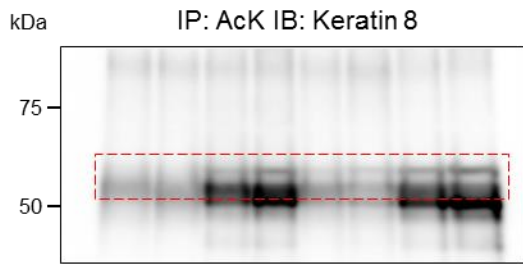
t



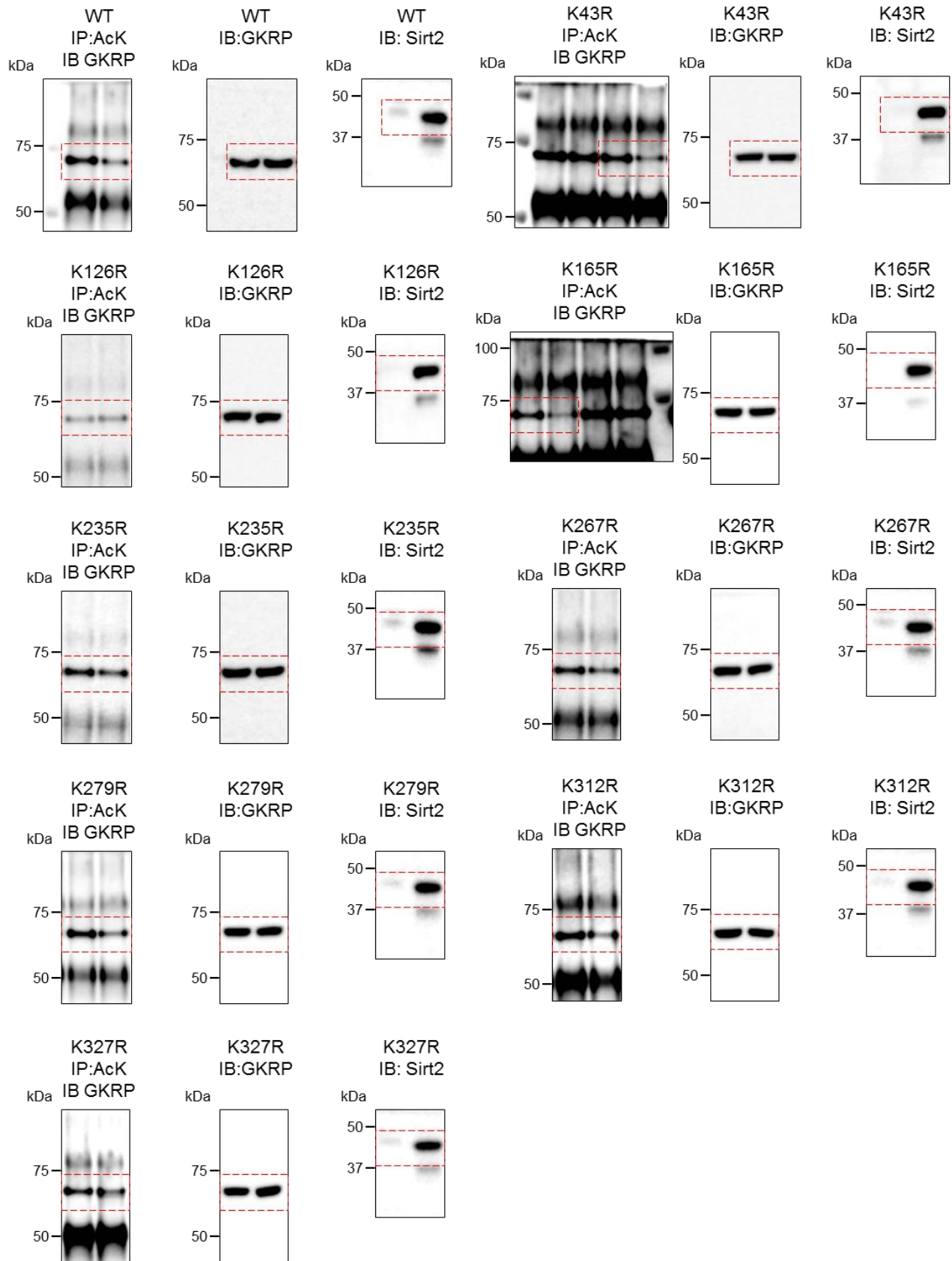
U



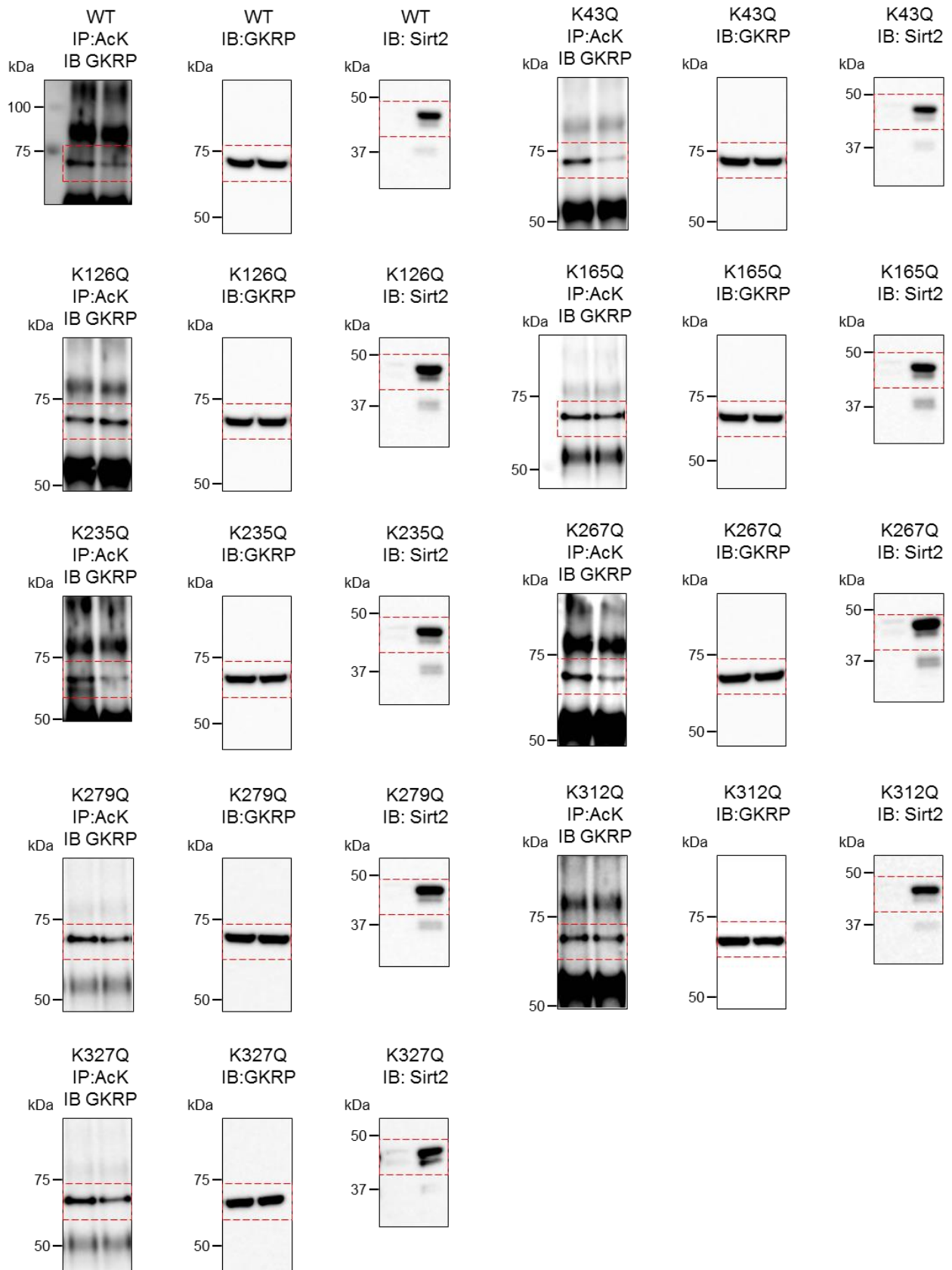
V



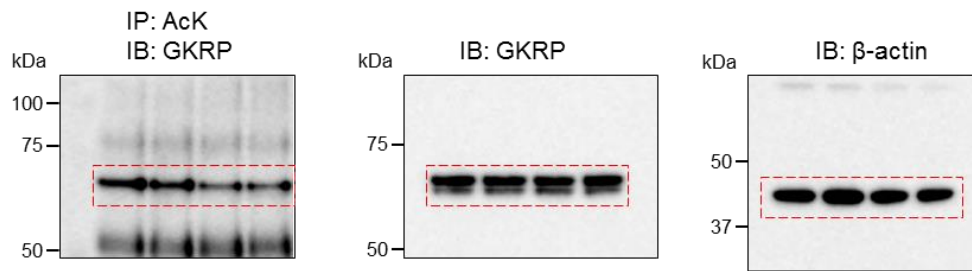
W



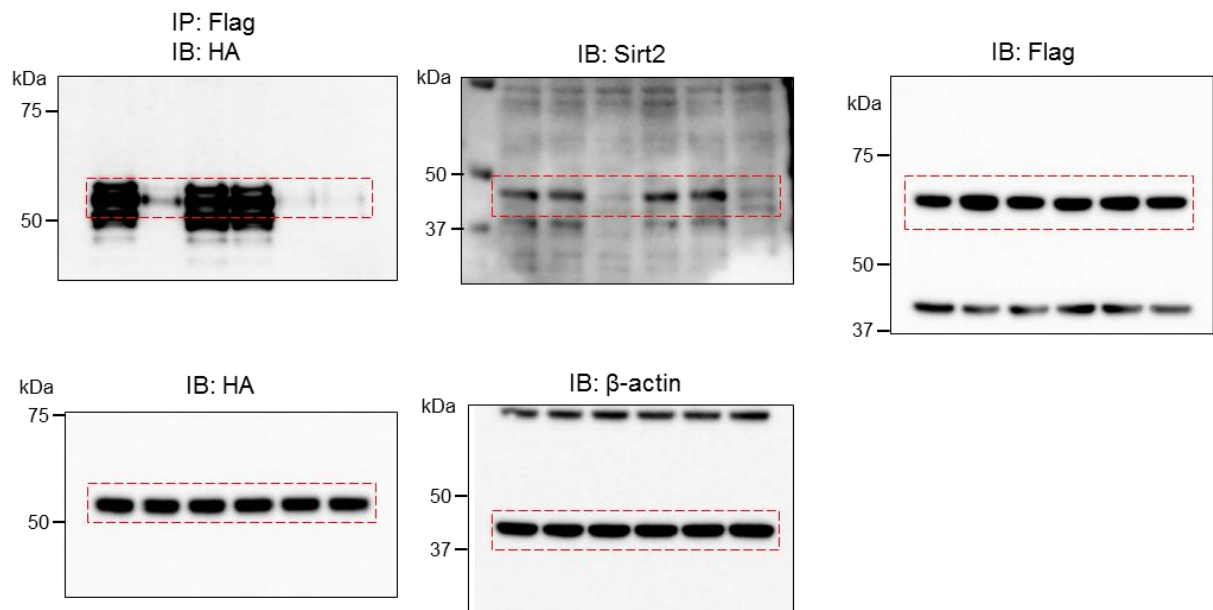
X



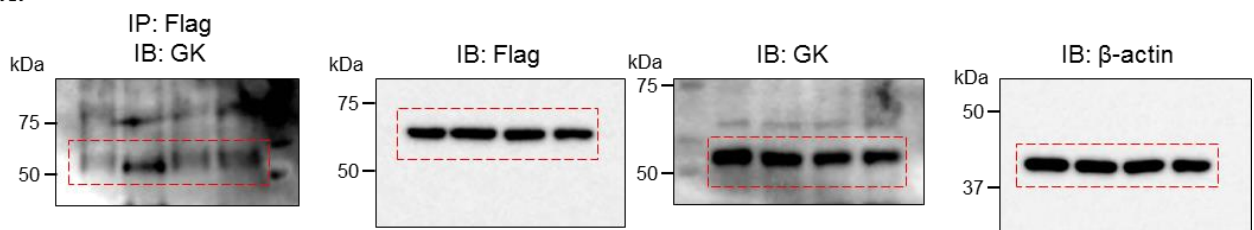
y



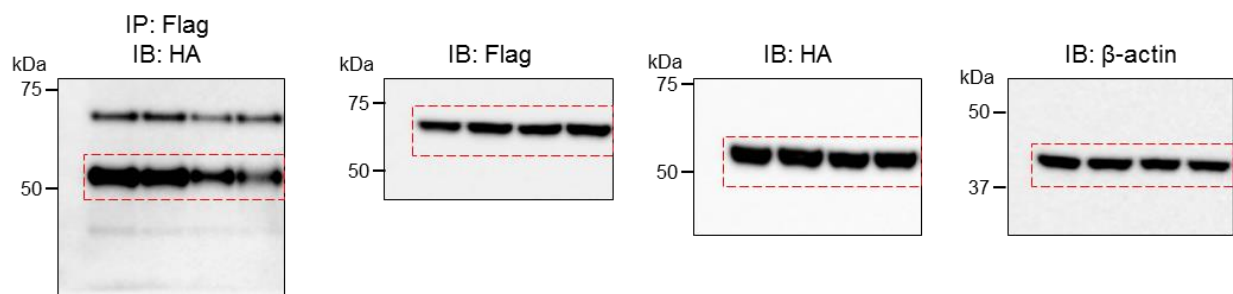
Z



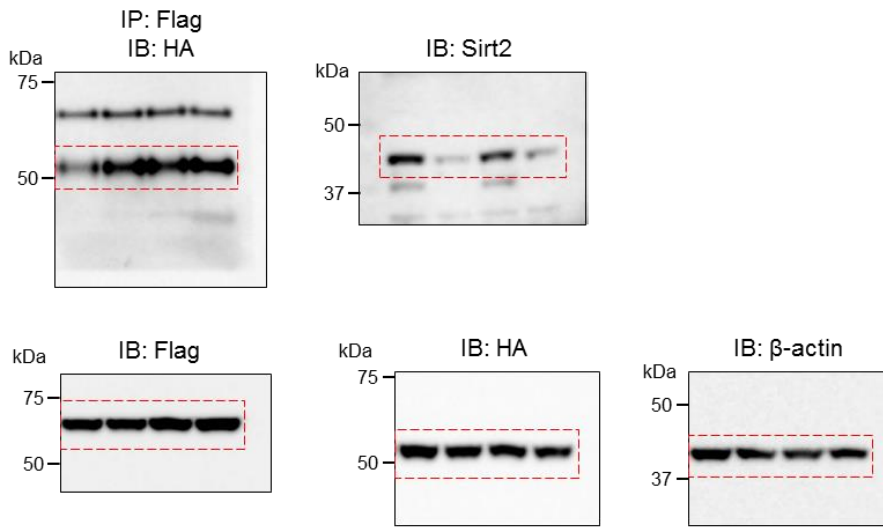
aa



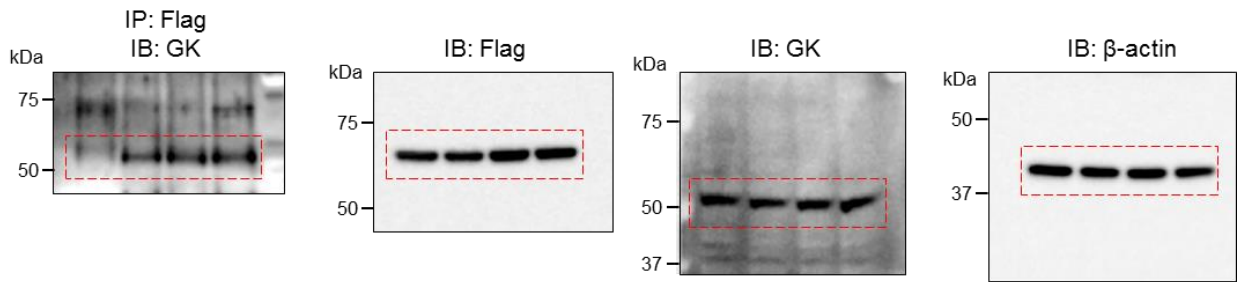
ab



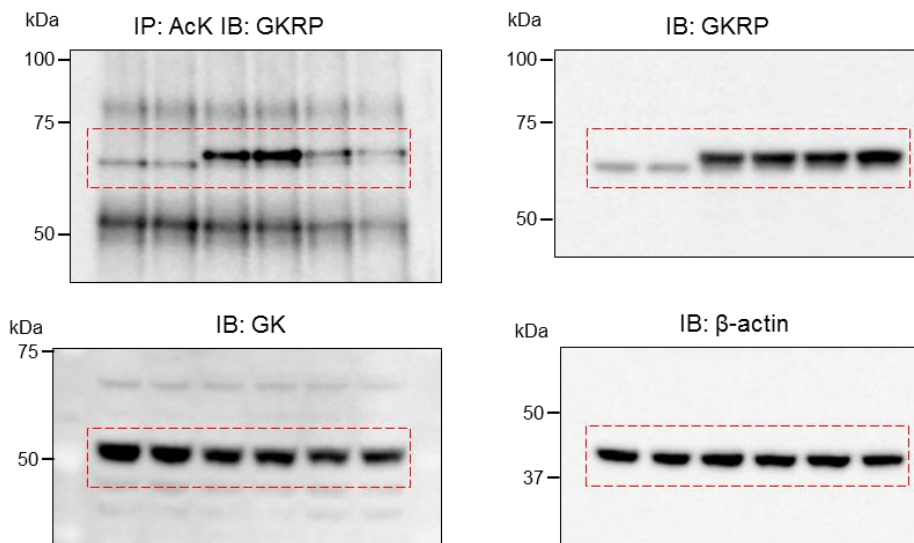
ac



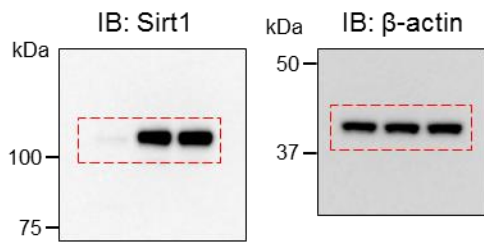
ad



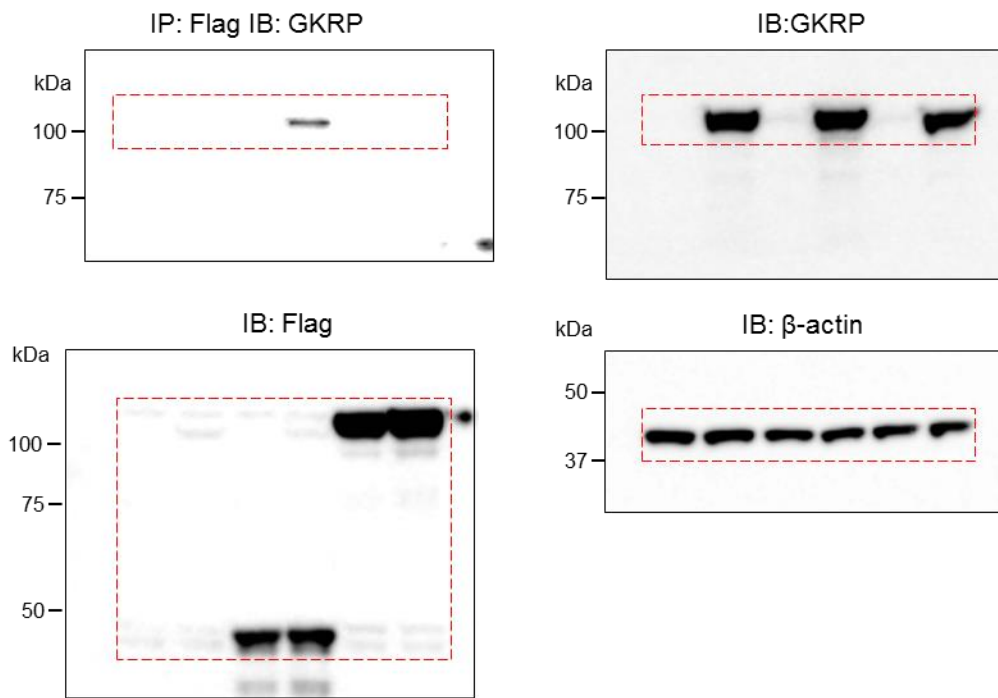
ae



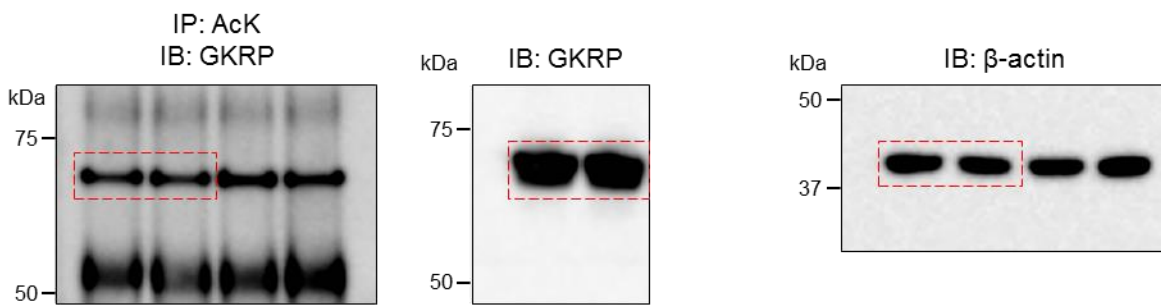
af



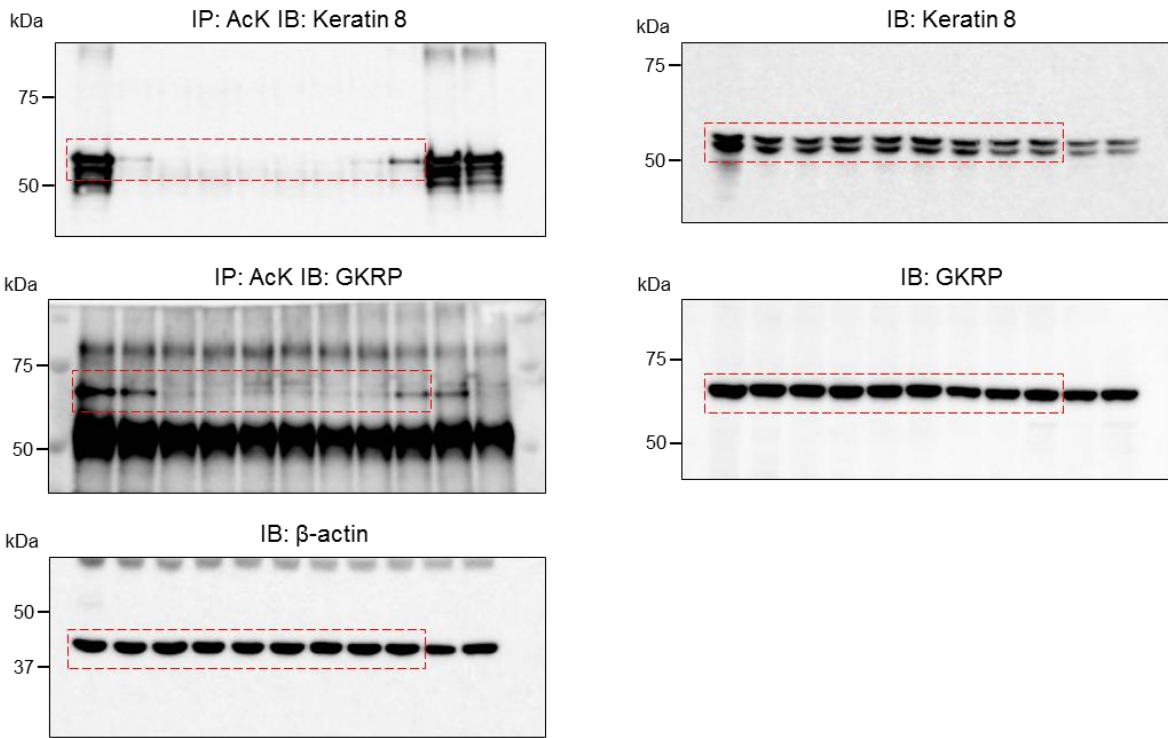
ag



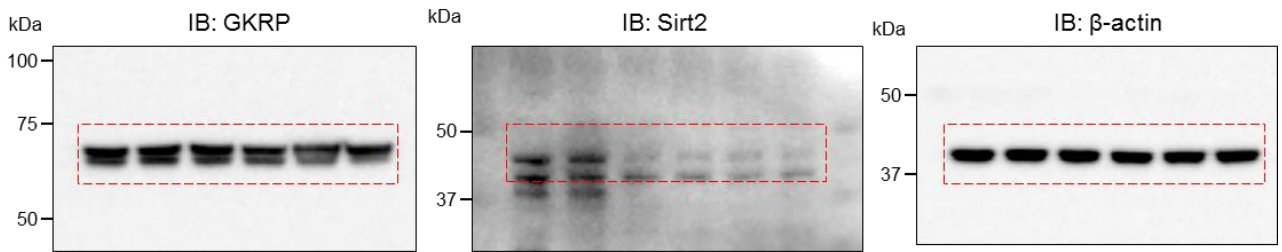
ah



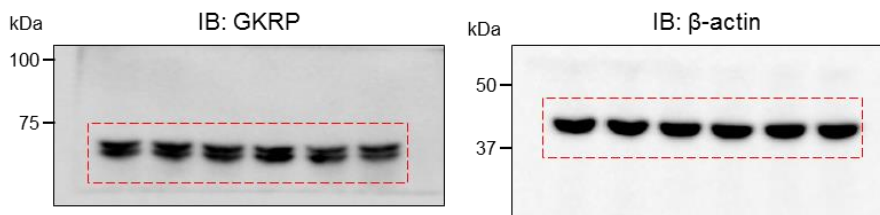
ai



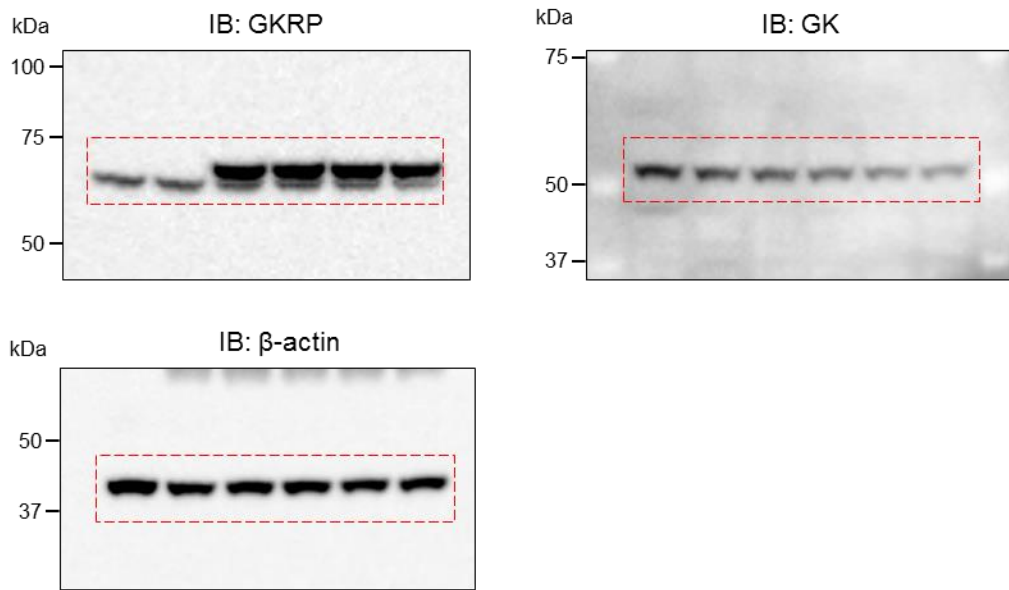
aj



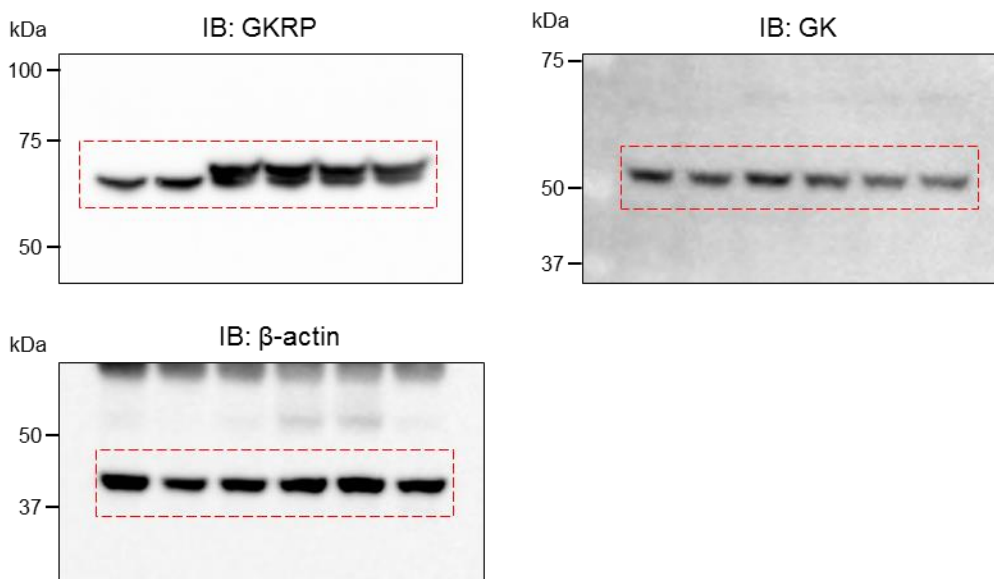
ak



**al**



**am**



**Supplementary Figure 9. Uncropped images of original scans of representative immunoblots.**

Uncropped versions of (a) Fig. 1d, (b) Fig. 1m, (c) Fig. 2c, (d) Fig. 2d, (e) Fig. 2e, (f) Fig. 2f, (g) Fig. 2g, (h) Fig. 2k, (i) Fig. 3a, (j) Fig. 3b, (k) Fig. 3c, (l) Fig. 3d, (m) Fig. 3f, (n) Fig. 3g, (o) Fig. 4a, (p) Fig. 4b, (q) Fig. 4c, (r) Fig. 4d, (s) Fig. 4e, (t) Fig. 4f, (u) Fig. 4g, (v) Fig. 4h, (w) Fig. 5a, (x) Fig. 5b, (y) Fig. 5c, (z) Fig. 5d, (aa) Fig. 5e, (ab) Fig. 5h, (ac) Fig. 5k, (ad) Fig. 5l, (ae) Fig. 7p, (af) Supplementary Fig. 3b, (ag) Supplementary Fig. 4a, (ah) Supplementary Fig. 4c, (ai) Supplementary Fig. 4d, (aj) Supplementary Fig. 6a, (ak) Supplementary Fig. 6b, (al) Supplementary Fig. 7a, (am) Supplementary Fig. 7e.